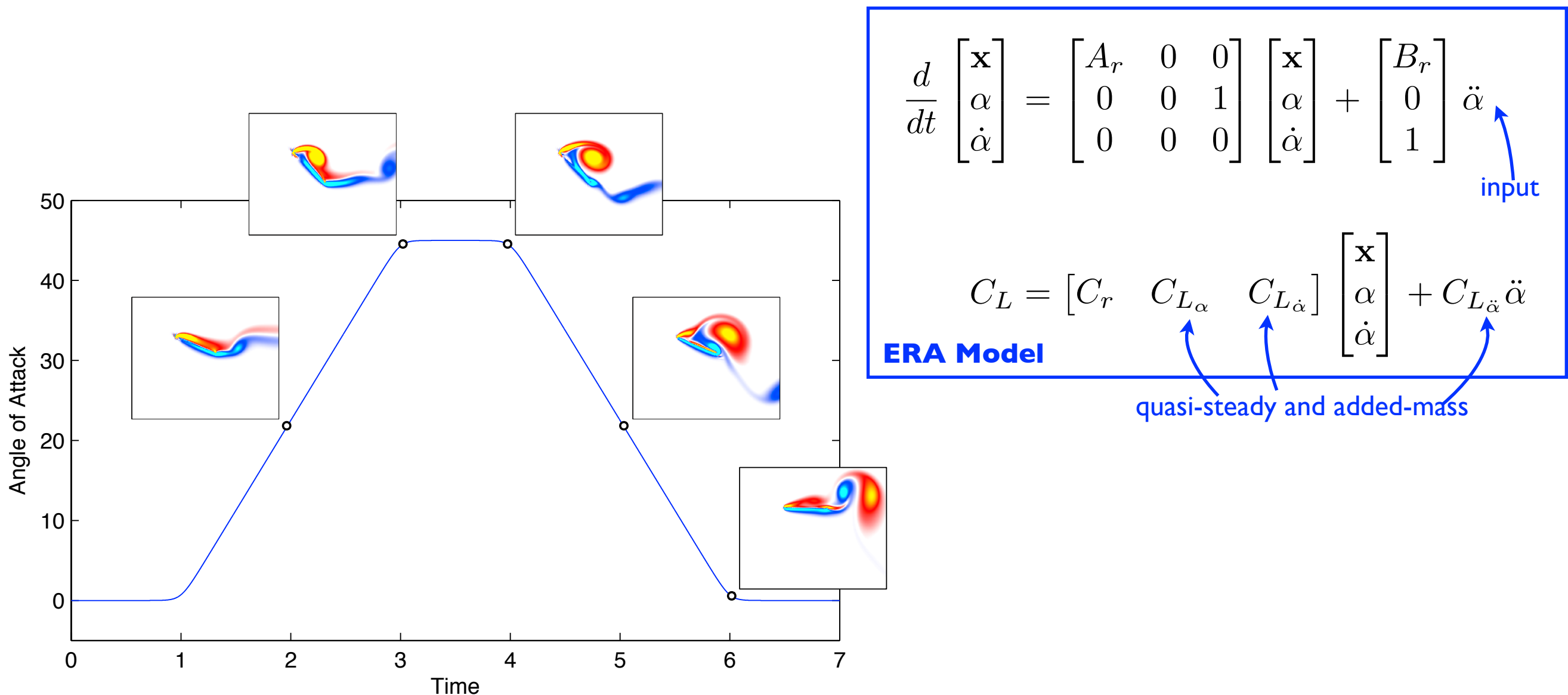


Low-dimensional state-space representations for classical unsteady aerodynamic models



Steve Brunton & Clancy Rowley
Princeton University
49th AIAA ASM January 6, 2011





Motivation



Applications of Unsteady Models

Conventional UAVs (performance/robustness)

Micro air vehicles (MAVs)

Flow control, flight dynamic control

Autopilots / Flight simulators

Gust disturbance mitigation

Understand bird/insect flight

Need for State-Space Models

Need models suitable for control

Combining with flight models

FLYIT Simulators, Inc.



Predator (General Atomics)



Bio-locomotion



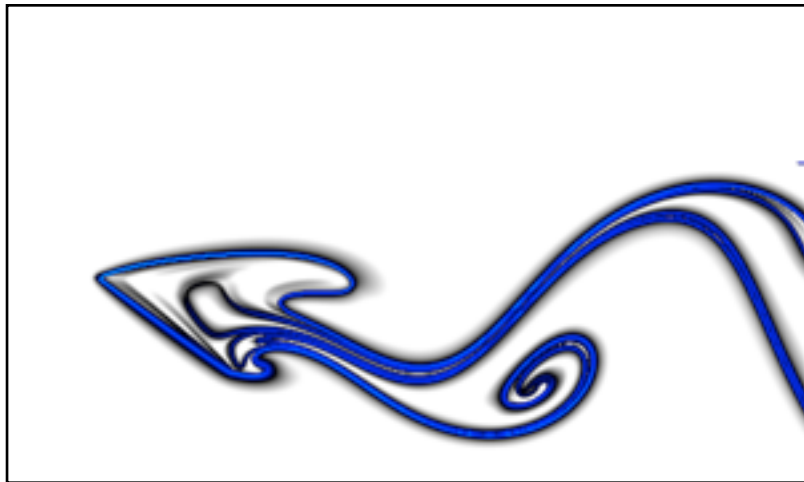
**Flexible Wing
(University of Florida)**



3 Types of Unsteadiness



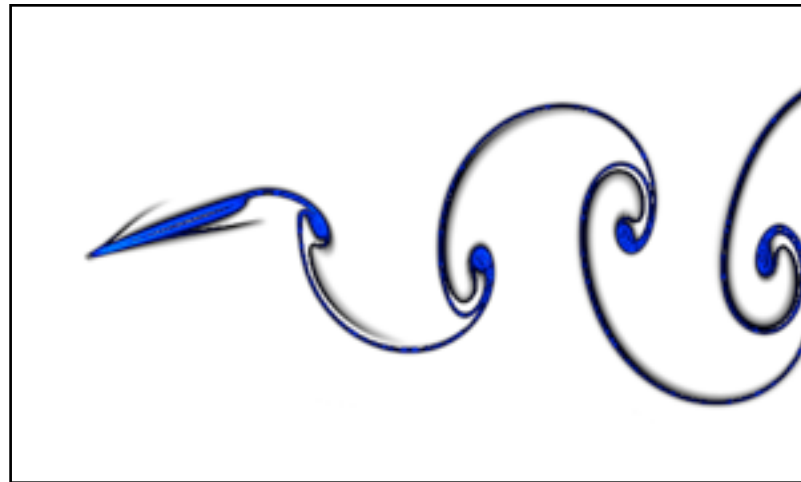
1. High angle-of-attack



$$\alpha > \alpha_{\text{stall}}$$

Large amplitude, slow

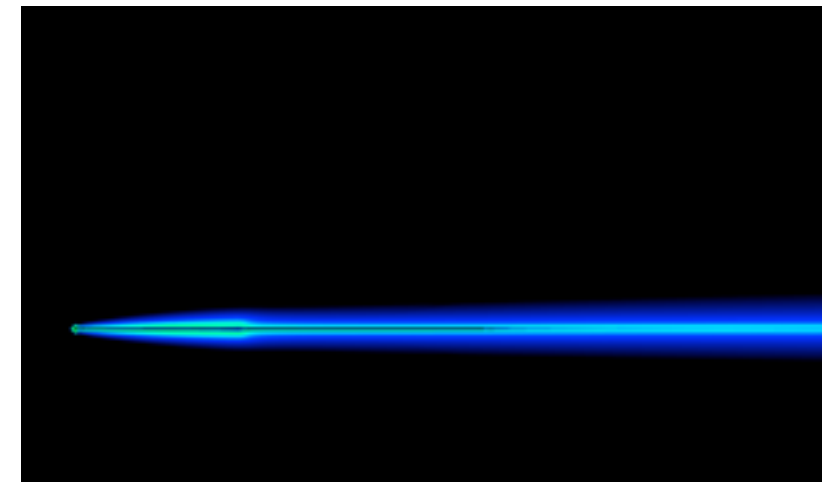
2. Strouhal number



$$St = \frac{Af}{U_\infty}$$

Moderate amplitude, fast

3. Reduced frequency



$$k = \frac{\pi fc}{U_\infty}$$

Small amplitude, very fast

Closely related

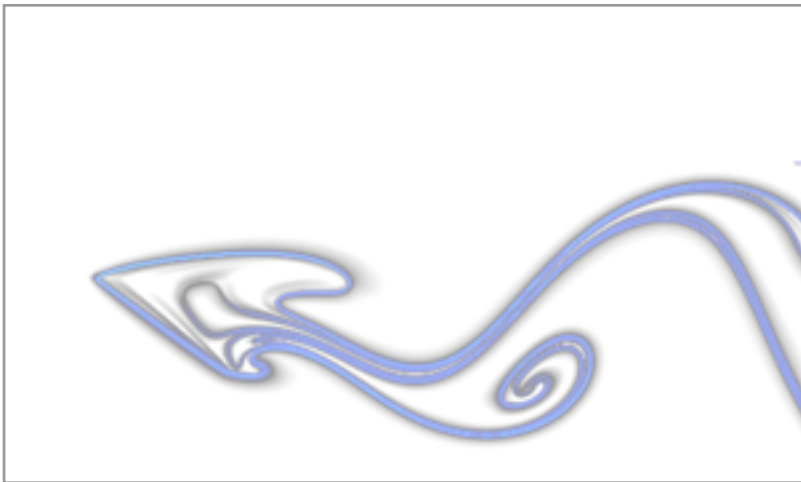
$$\alpha_{\text{eff}} = \tan^{-1}(\pi St)$$



3 Types of Unsteadiness



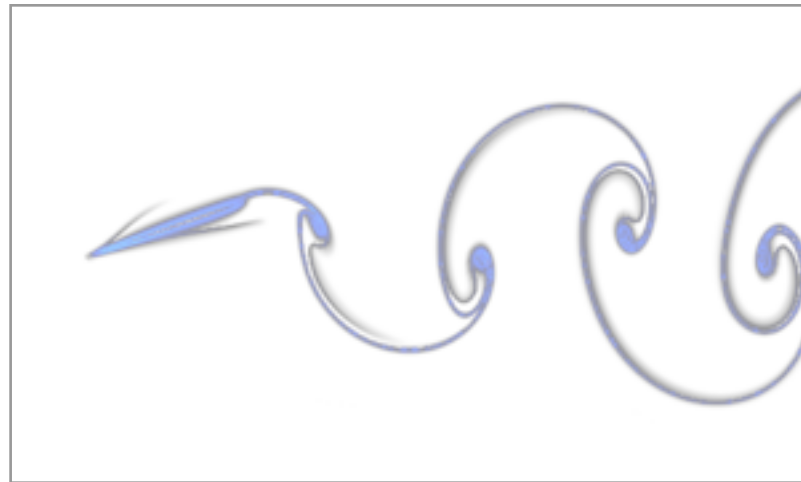
1. High angle-of-attack



$$\alpha > \alpha_{\text{stall}}$$

Large amplitude, slow

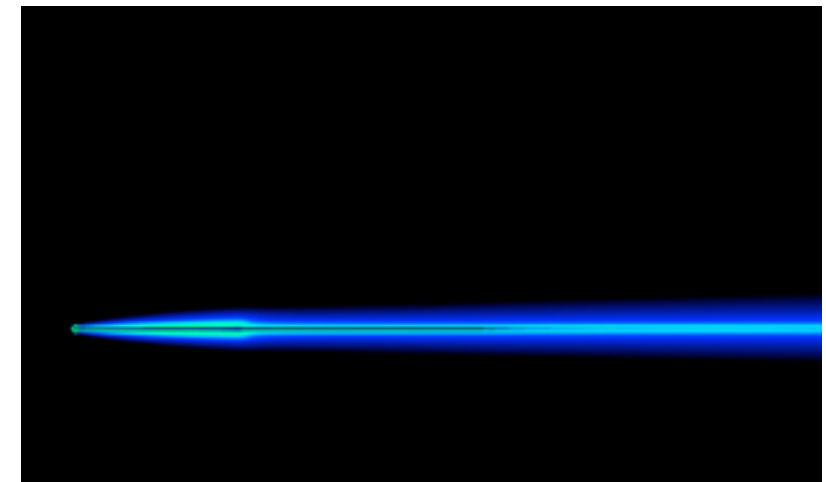
2. Strouhal number



$$St = \frac{Af}{U_\infty}$$

Moderate amplitude, fast

3. Reduced frequency



$$k = \frac{\pi fc}{U_\infty}$$

Small amplitude, very fast

Closely related

$$\alpha_{\text{eff}} = \tan^{-1}(\pi St)$$



Candidate Lift Models



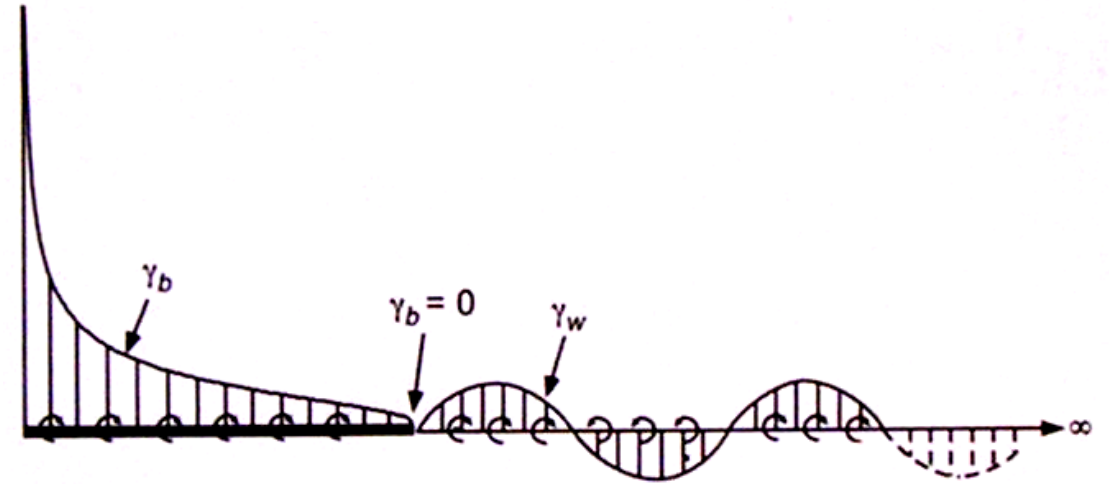
$$C_L = 2\pi\alpha$$

$$C_L = C_{L_\alpha} \alpha$$

$$C_L = C_L(\alpha)$$

$$C_L(t) = C_L^\delta(t)\alpha(0) + \int_0^t C_L^\delta(t - \tau)\dot{\alpha}(\tau)d\tau$$

Wagner's Indicial Response



$$C_L = \underbrace{\frac{\pi}{2} \left[\ddot{h} + \dot{\alpha} - \frac{a}{2}\ddot{\alpha} \right]}_{\text{Added-Mass}} + \underbrace{2\pi \left[\alpha + \dot{h} + \frac{1}{2}\dot{\alpha} \left(\frac{1}{2} - a \right) \right]}_{\text{Circulatory}} C(k)$$

Theodorsen's Model

Motivation for State-Space Models

Captures input output dynamics accurately

Computationally tractable

fits into control framework

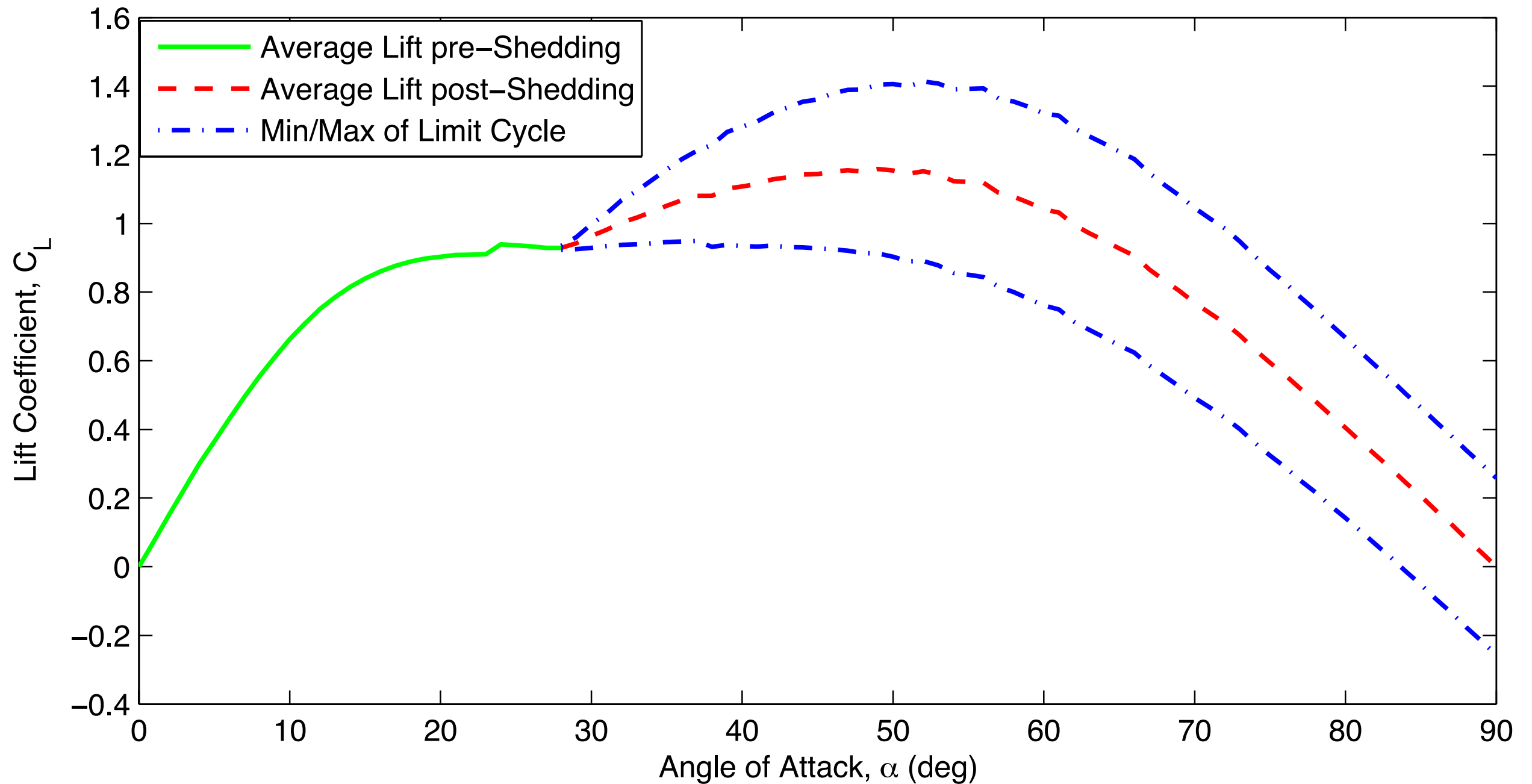
Wagner, 1925.

Theodorsen, 1935.

Leishman, 2006.



Lift vs Angle of Attack



Low Reynolds number, (Re=100)

Hopf bifurcation at $\alpha_{crit} \approx 28^\circ$

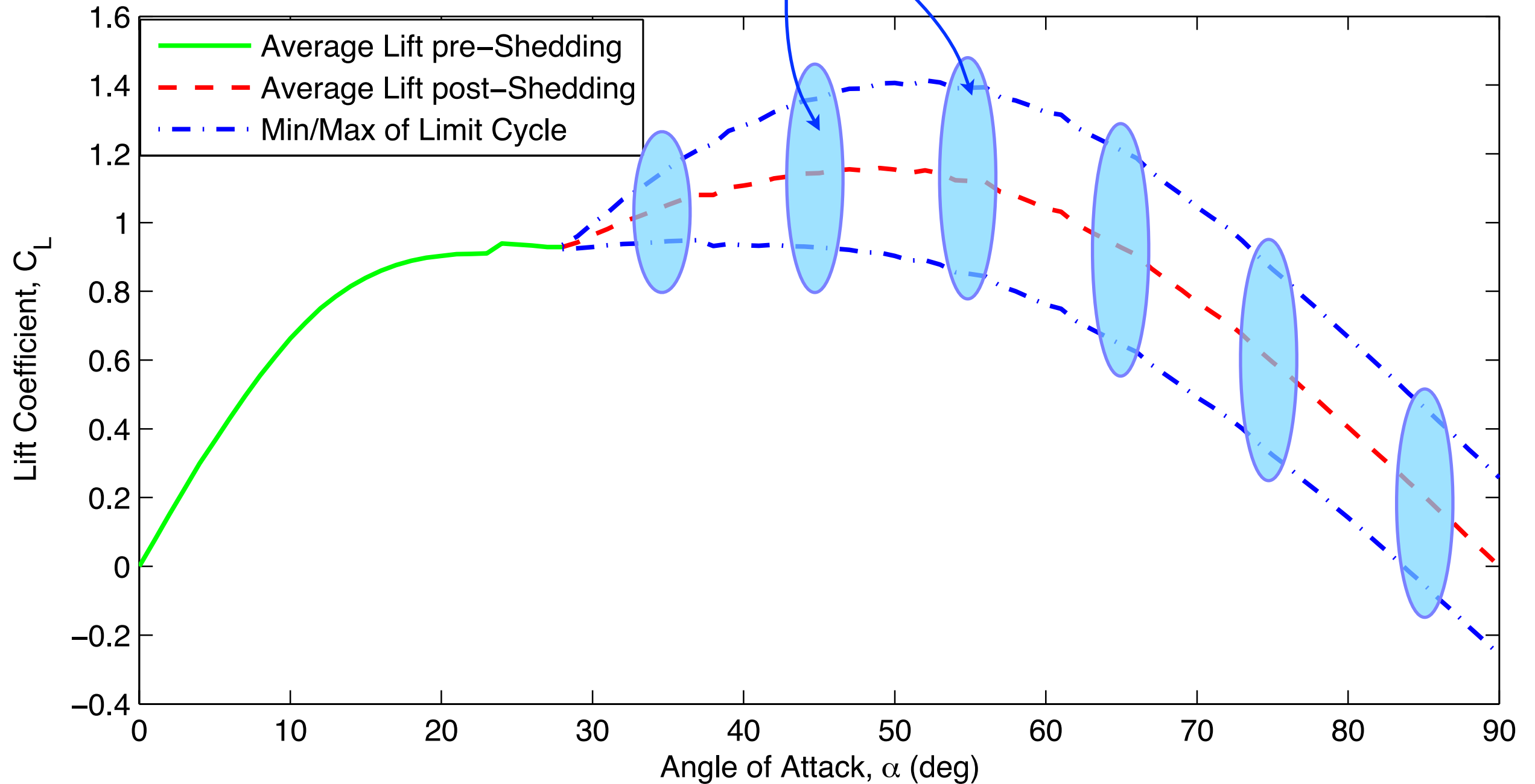
(pair of imaginary eigenvalues pass into right half plane)



Lift vs Angle of Attack



Models based on Hopf normal form capture vortex shedding



Low Reynolds number, (Re=100)

Hopf bifurcation at $\alpha_{crit} \approx 28^\circ$

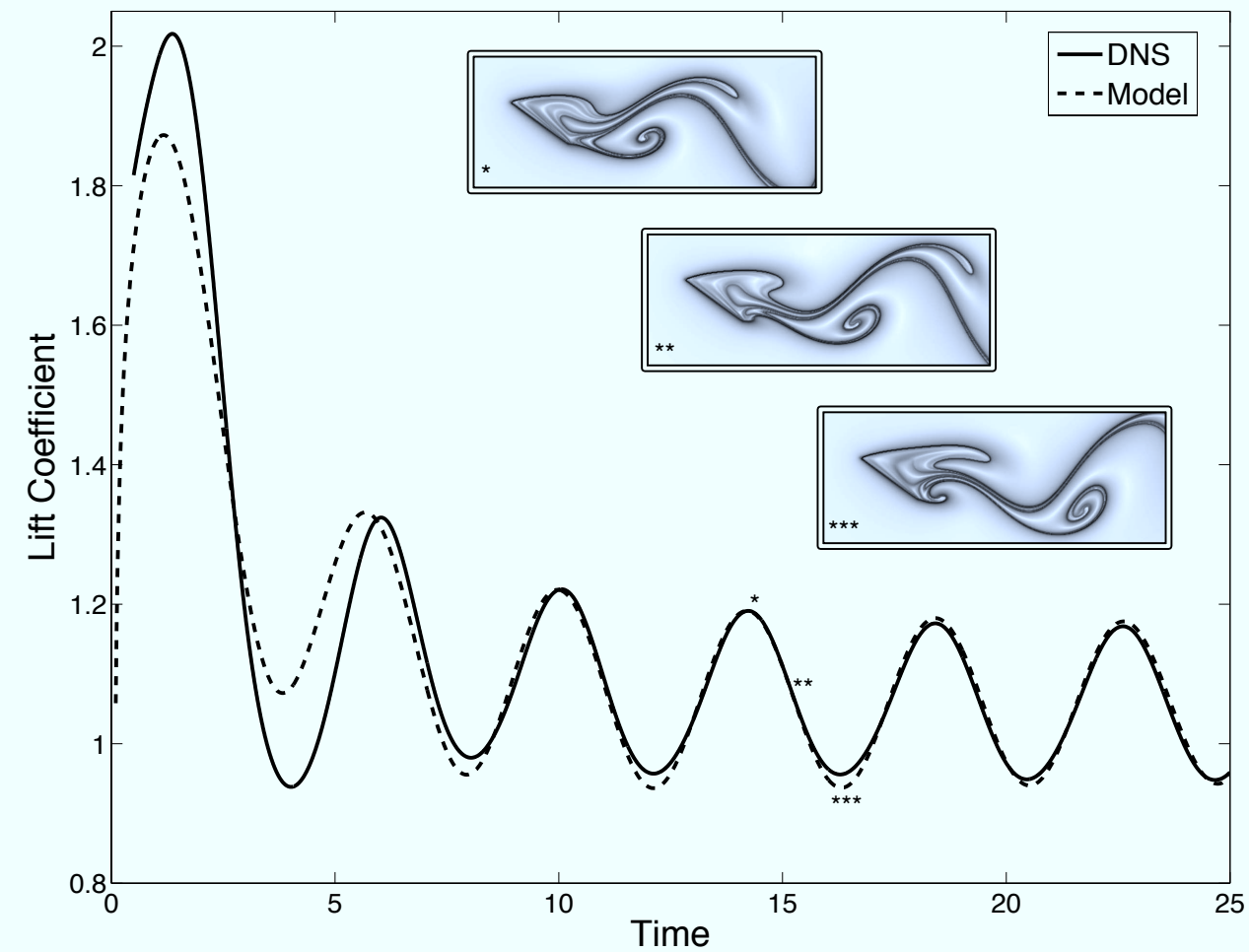
(pair of imaginary eigenvalues pass into right half plane)



High angle of attack models



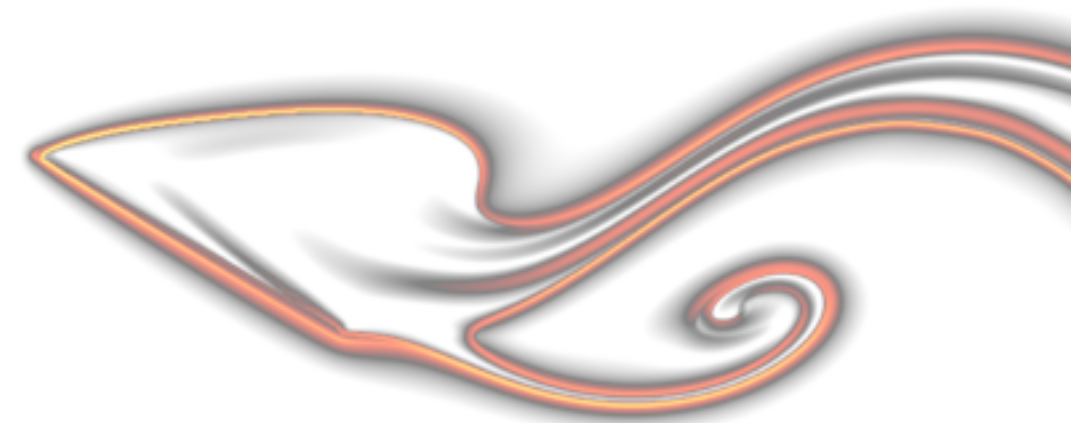
Heuristic Model



Galerkin Projection onto POD



Full DNS



Reconstruction

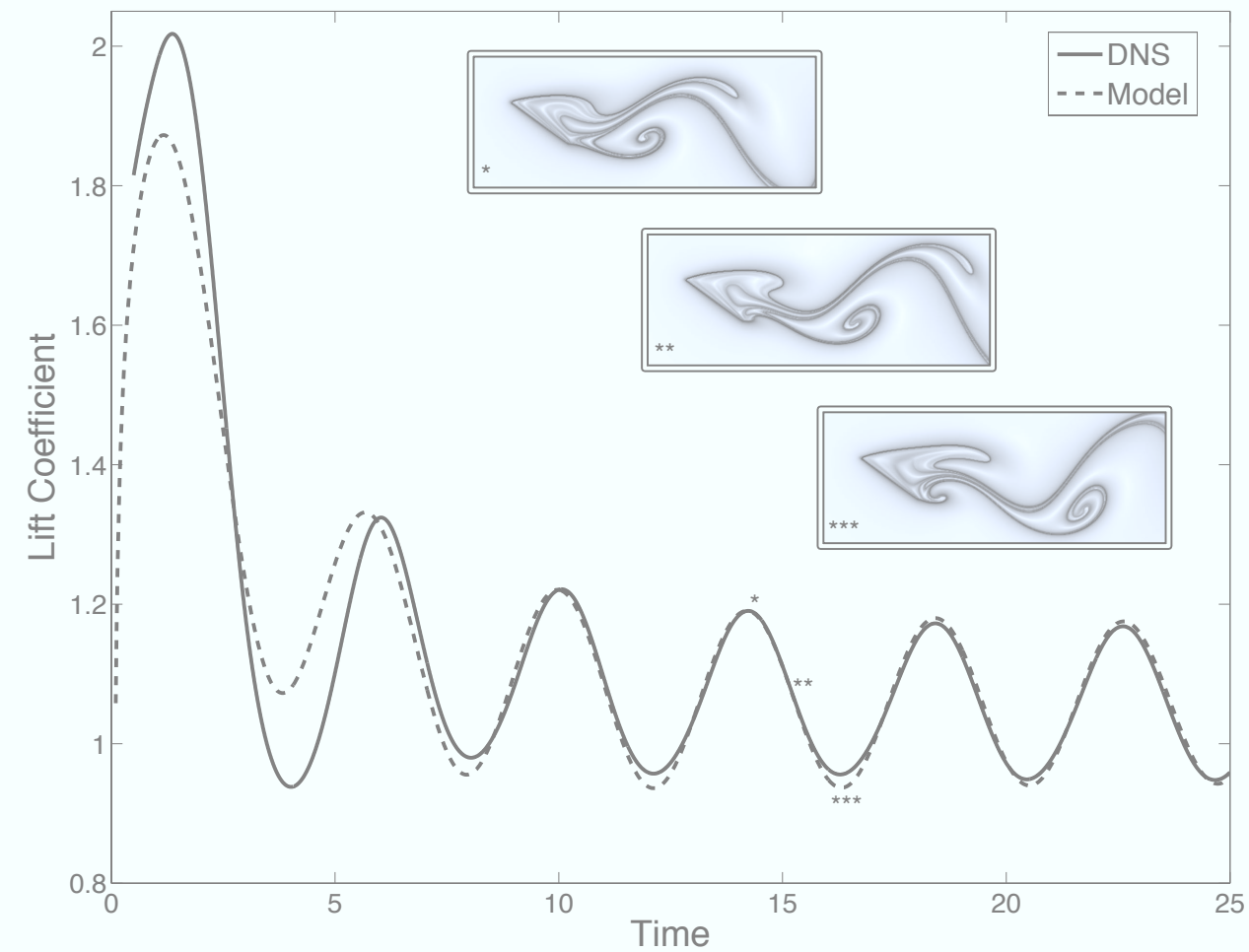
$$\left. \begin{aligned} \dot{x} &= (\alpha - \alpha_c)\mu x - \omega y - ax(x^2 + y^2) \\ \dot{y} &= (\alpha - \alpha_c)\mu y + \omega x - ay(x^2 + y^2) \\ \dot{z} &= -\lambda z \end{aligned} \right\} \implies \begin{aligned} \dot{r} &= r [(\alpha - \alpha_c)\mu - ar^2] \\ \dot{\theta} &= \omega \\ \dot{z} &= -\lambda z \end{aligned}$$



High angle of attack models



Heuristic Model



Galerkin Projection onto POD



Full DNS

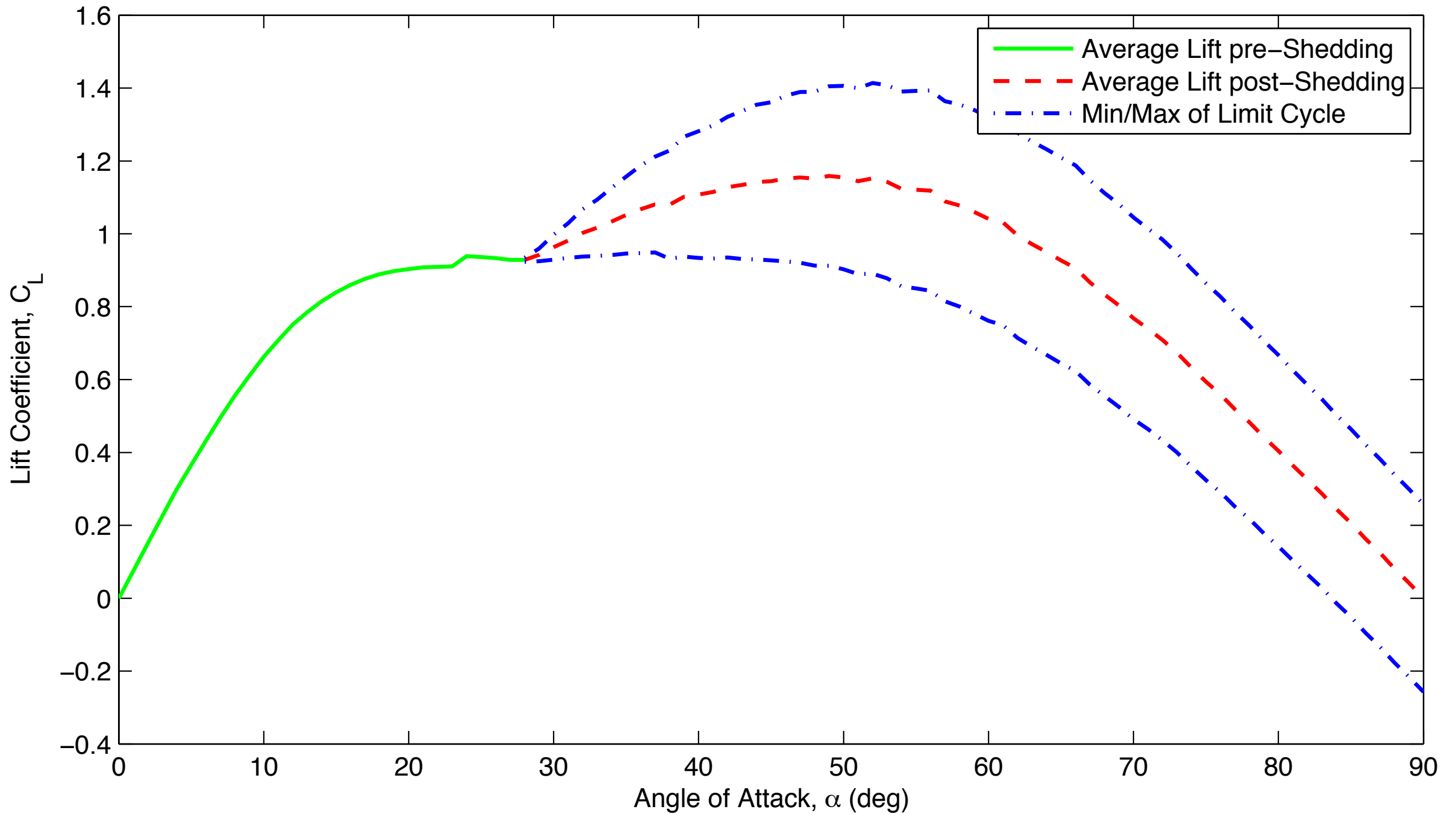


Reconstruction

$$\left. \begin{aligned} \dot{x} &= (\alpha - \alpha_c)\mu x - \omega y - ax(x^2 + y^2) \\ \dot{y} &= (\alpha - \alpha_c)\mu y + \omega x - ay(x^2 + y^2) \\ \dot{z} &= -\lambda z \end{aligned} \right\} \Rightarrow \begin{aligned} \dot{r} &= r [(\alpha - \alpha_c)\mu - ar^2] \\ \dot{\theta} &= \omega \\ \dot{z} &= -\lambda z \end{aligned}$$



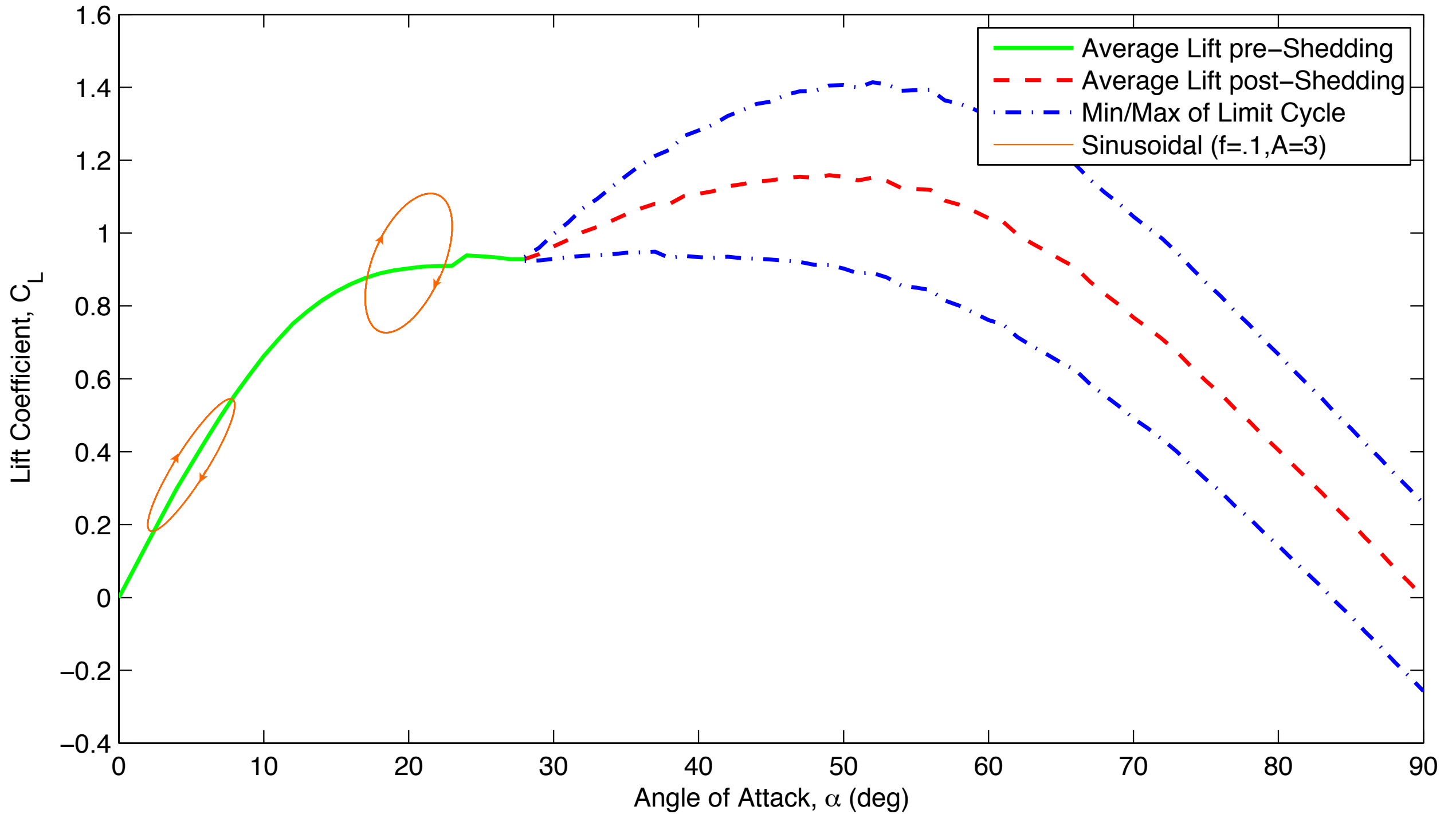
Lift vs. Angle of Attack



Need model that captures lift due to moving airfoil!



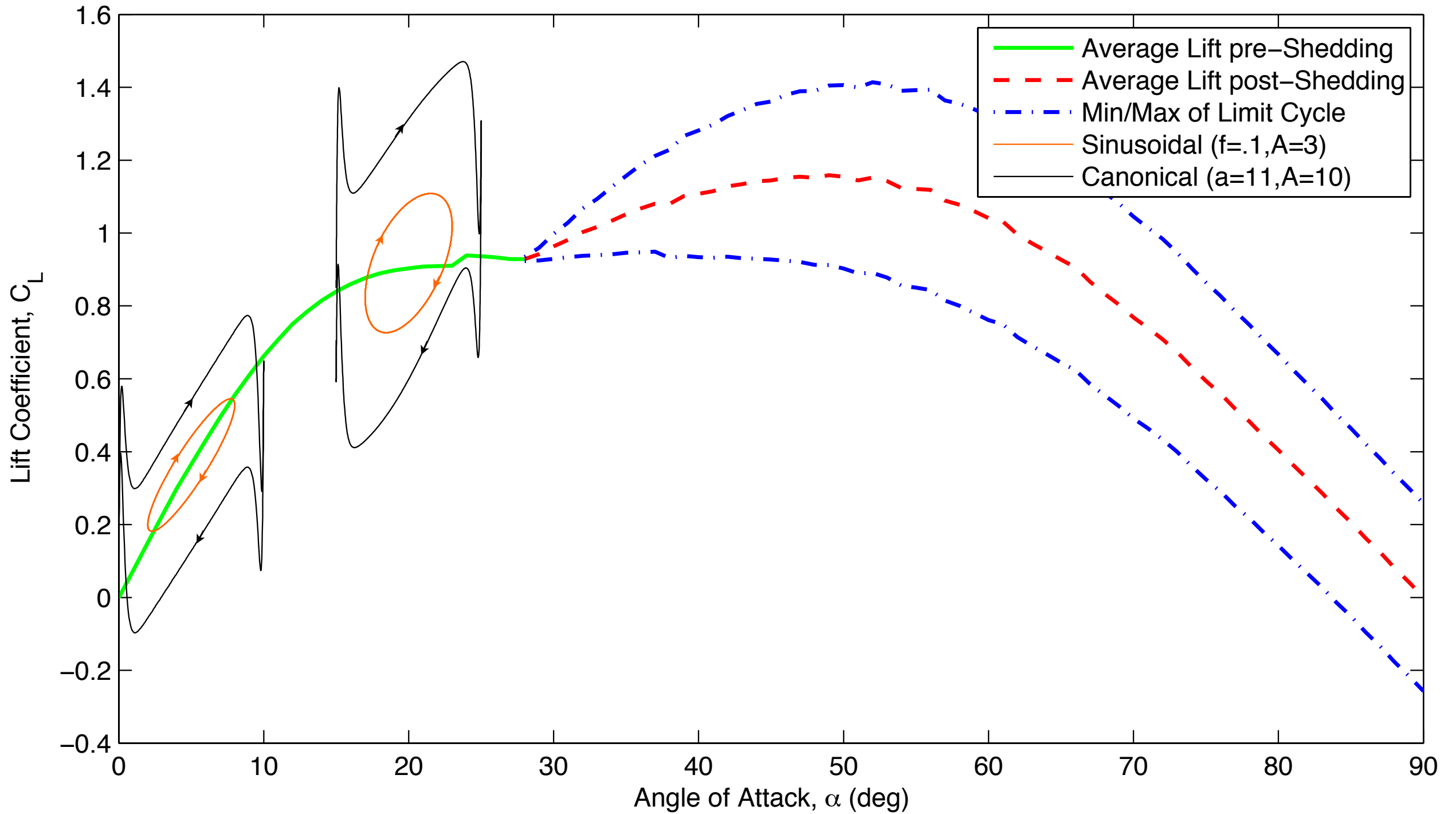
Lift vs. Angle of Attack



Need model that captures lift due to moving airfoil!



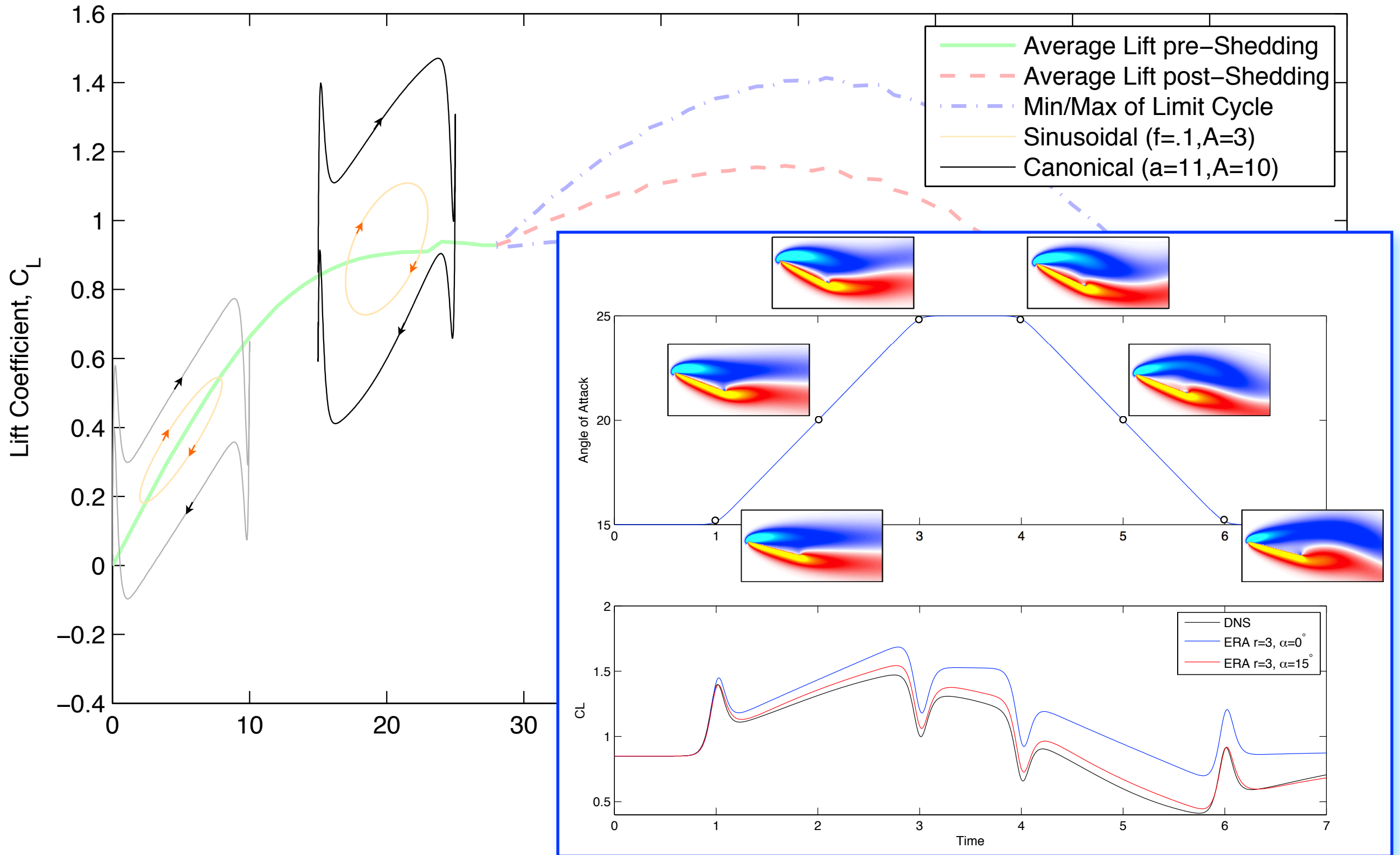
Lift vs. Angle of Attack



Need model that captures lift due to moving airfoil!



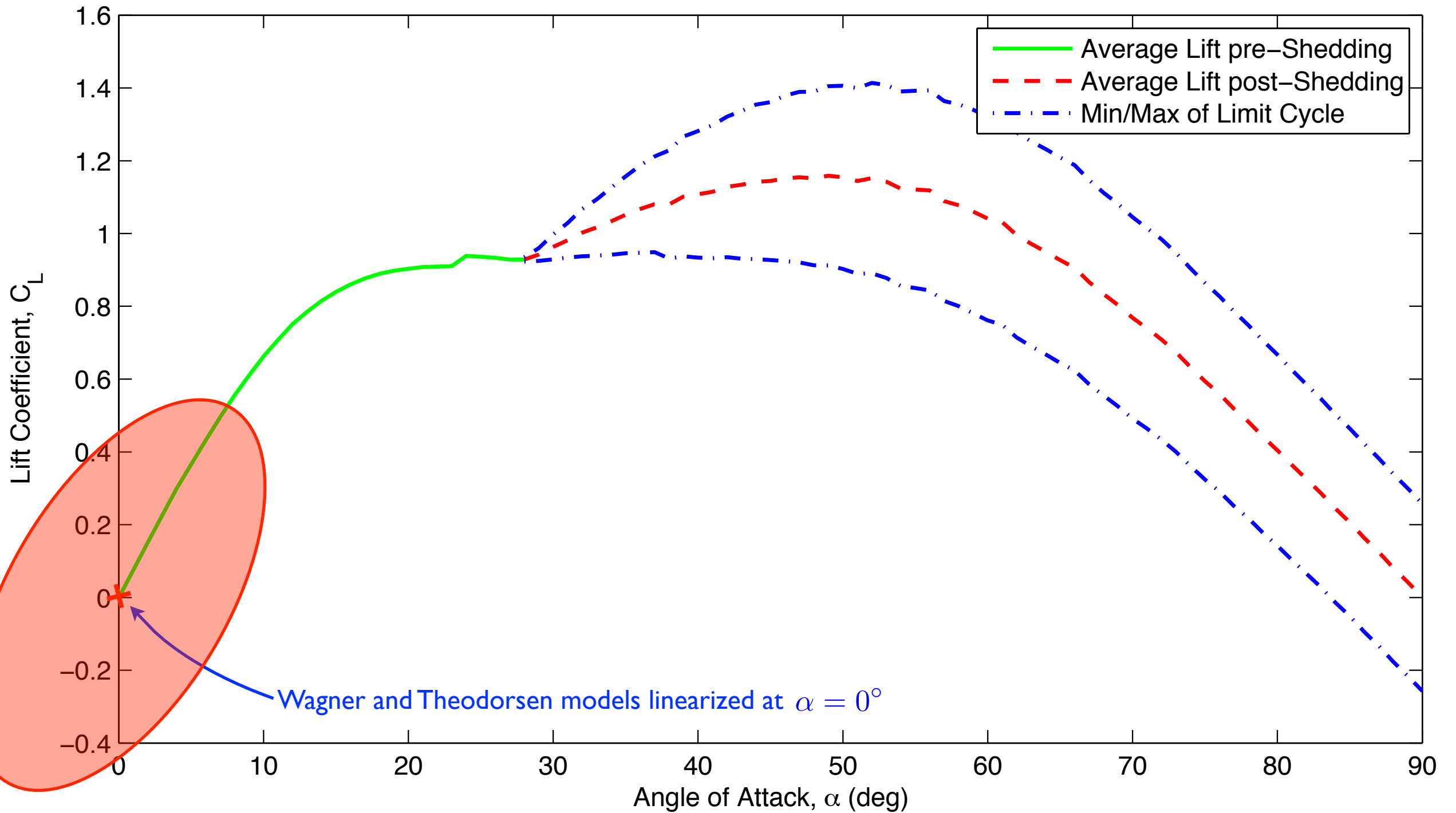
Lift vs. Angle of Attack



Need model that captures lift due to moving airfoil!



Lift vs. Angle of Attack

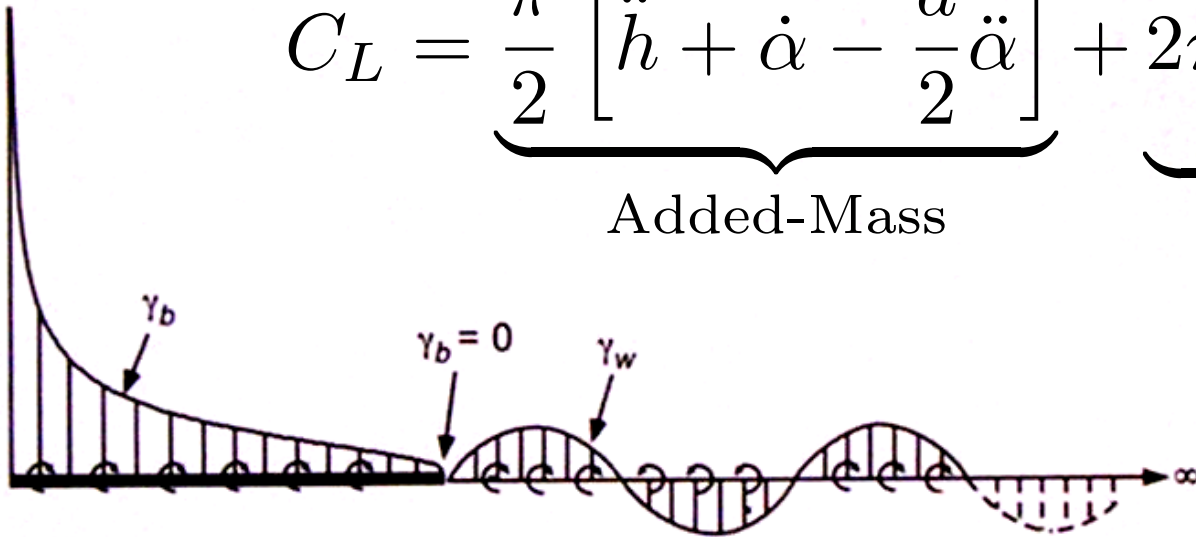




Theodorsen's Model



$$C_L = \underbrace{\frac{\pi}{2} \left[\ddot{h} + \dot{\alpha} - \frac{a}{2} \ddot{\alpha} \right]}_{\text{Added-Mass}} + \underbrace{2\pi \left[\alpha + \dot{h} + \frac{1}{2} \dot{\alpha} \left(\frac{1}{2} - a \right) \right]}_{\text{Circulatory}} C(k)$$



$$C(k) = \frac{H_1^{(2)}(k)}{H_1^{(2)}(k) + iH_0^{(2)}(k)}$$

2D Incompressible, inviscid model

Unsteady potential flow (w/ Kutta condition)

Linearized about zero angle of attack

$$k = \frac{\pi f c}{U_\infty}$$

Apparent Mass

Increasingly important for lighter aircraft

Not trivial to compute, but essentially solved

force needed to move air as plate accelerates

Circulatory Lift

Captures separation effects

Need improved models here

source of all lift in steady flight

Theodorsen, 1935.

Leishman, 2006.



Empirical Theodorsen



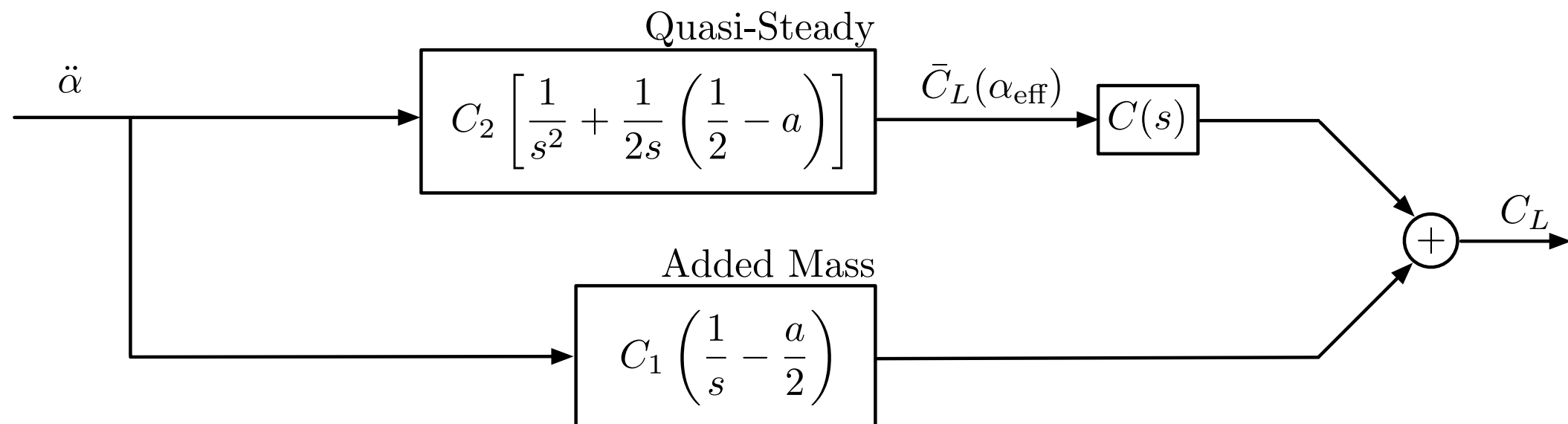
$$C_L = \underbrace{\frac{\pi}{2} \left[\ddot{h} + \dot{\alpha} - \frac{a}{2} \ddot{\alpha} \right]}_{\text{Added-Mass}} + \underbrace{2\pi \left[\alpha + \dot{h} + \frac{1}{2} \dot{\alpha} \left(\frac{1}{2} - a \right) \right]}_{\text{Circulatory}} C(k)$$

Generalized Coefficients

$$C_L = C_1 \left[\dot{\alpha} - \frac{a}{2} \ddot{\alpha} \right] + C_2 \left[\alpha + \frac{1}{2} \dot{\alpha} \left(\frac{1}{2} - a \right) \right] C(k)$$

Transfer Function

$$\frac{\mathcal{L}[C_L]}{\mathcal{L}[\ddot{\alpha}]} = C_1 \left(\frac{1}{s} - \frac{a}{2} \right) + C_2 \left[\frac{1}{s^2} + \frac{1}{2s} \left(\frac{1}{2} - a \right) \right] C(s)$$





Pade Approximate $C(k)$

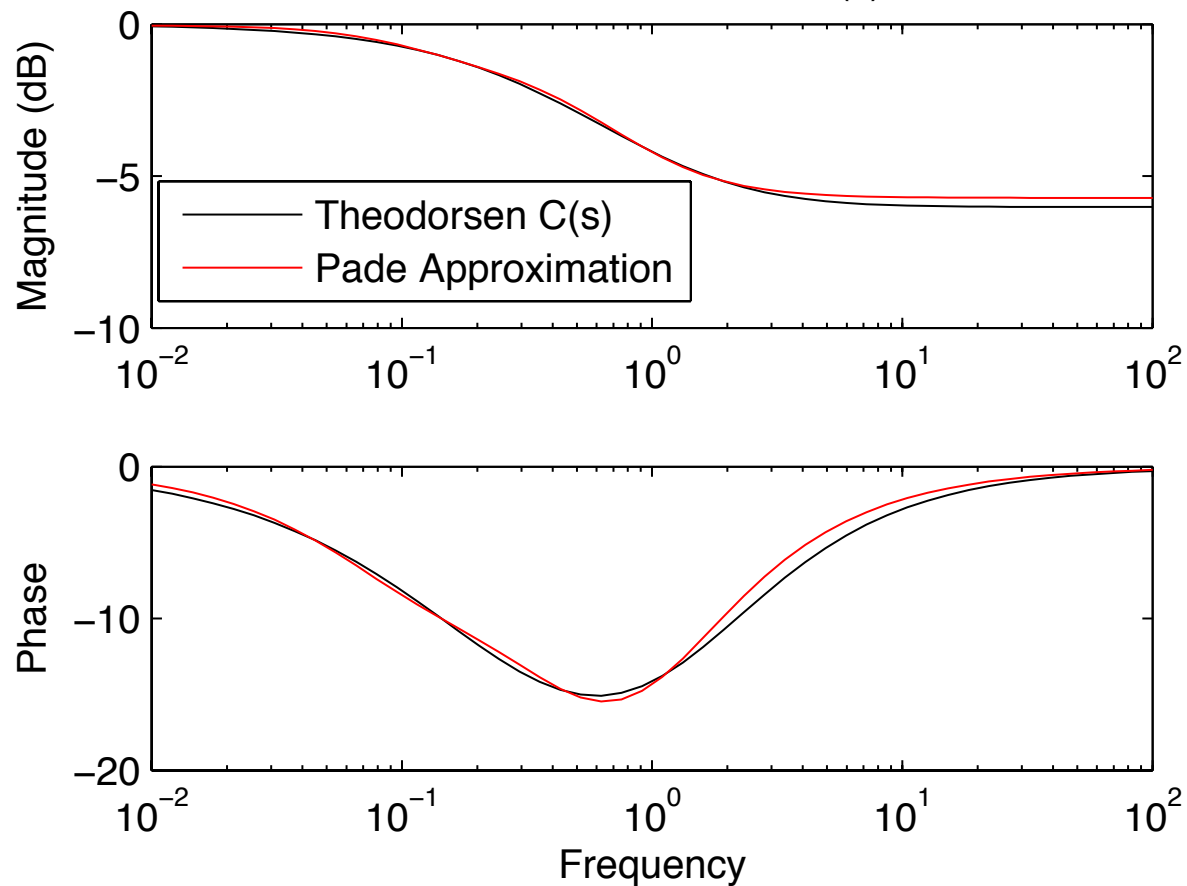


$$C(k) \approx .99612 - .1666 \frac{k}{k+.0553} - .3119 \frac{k}{k+.28606}$$

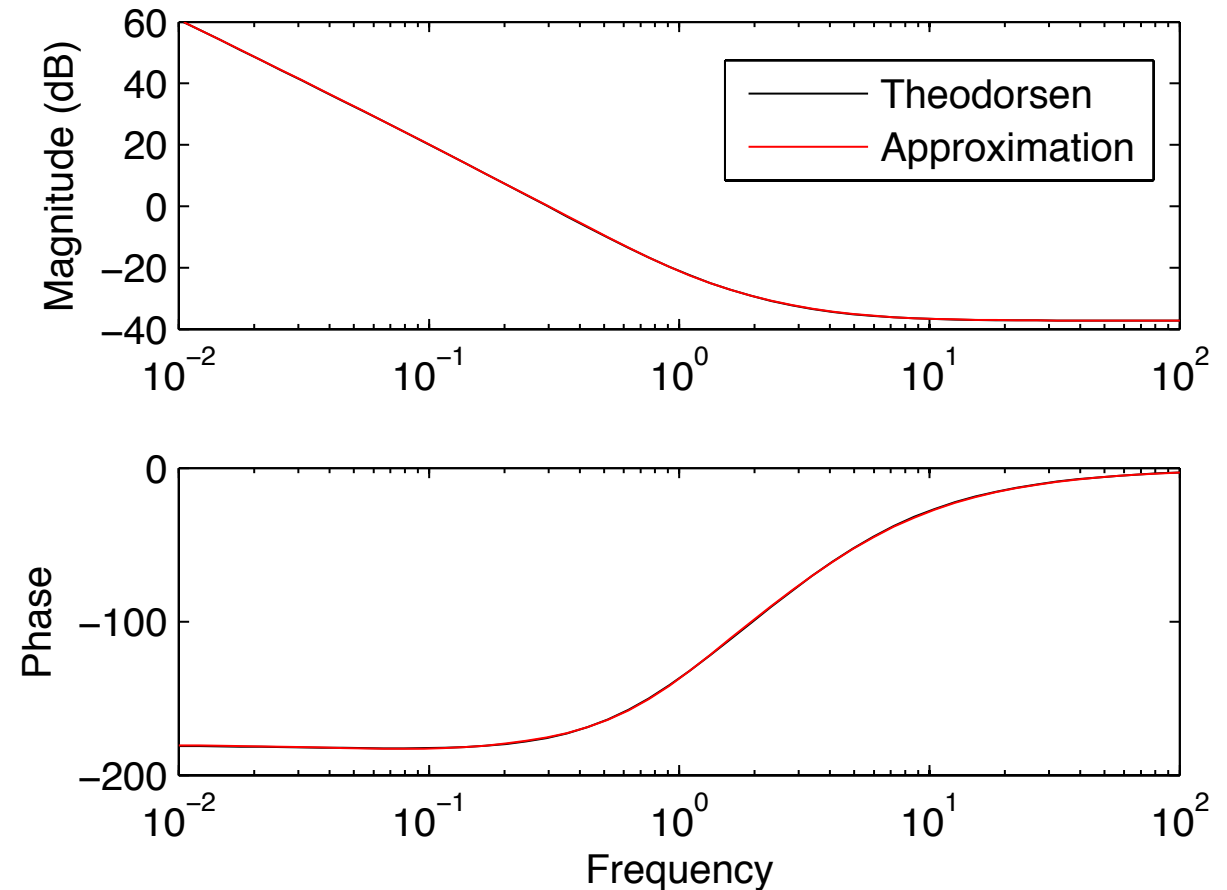
$$C(k) = \frac{H_1^{(2)}(k)}{H_1^{(2)}(k) + iH_0^{(2)}(k)}$$

$$C(s) \approx \frac{.1294s^2 + .1376s + .01576}{.25s^2 + .1707s + .01582}$$

Theodorsen Function $C(s)$ $s = 2k$

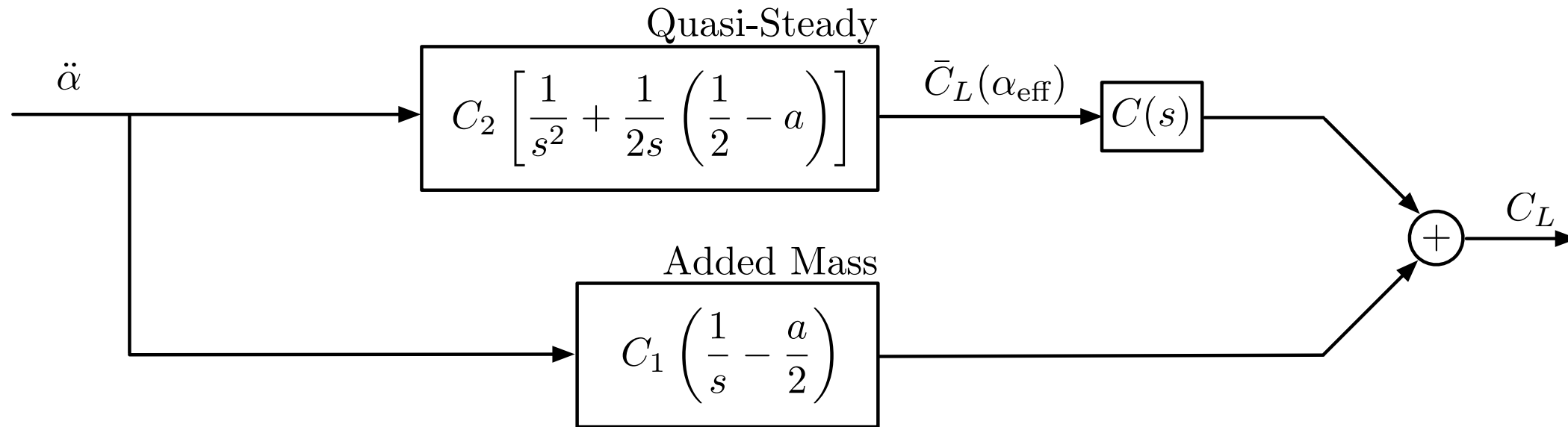


Lift Model (Leading Edge Pitch)





Empirical C(s)

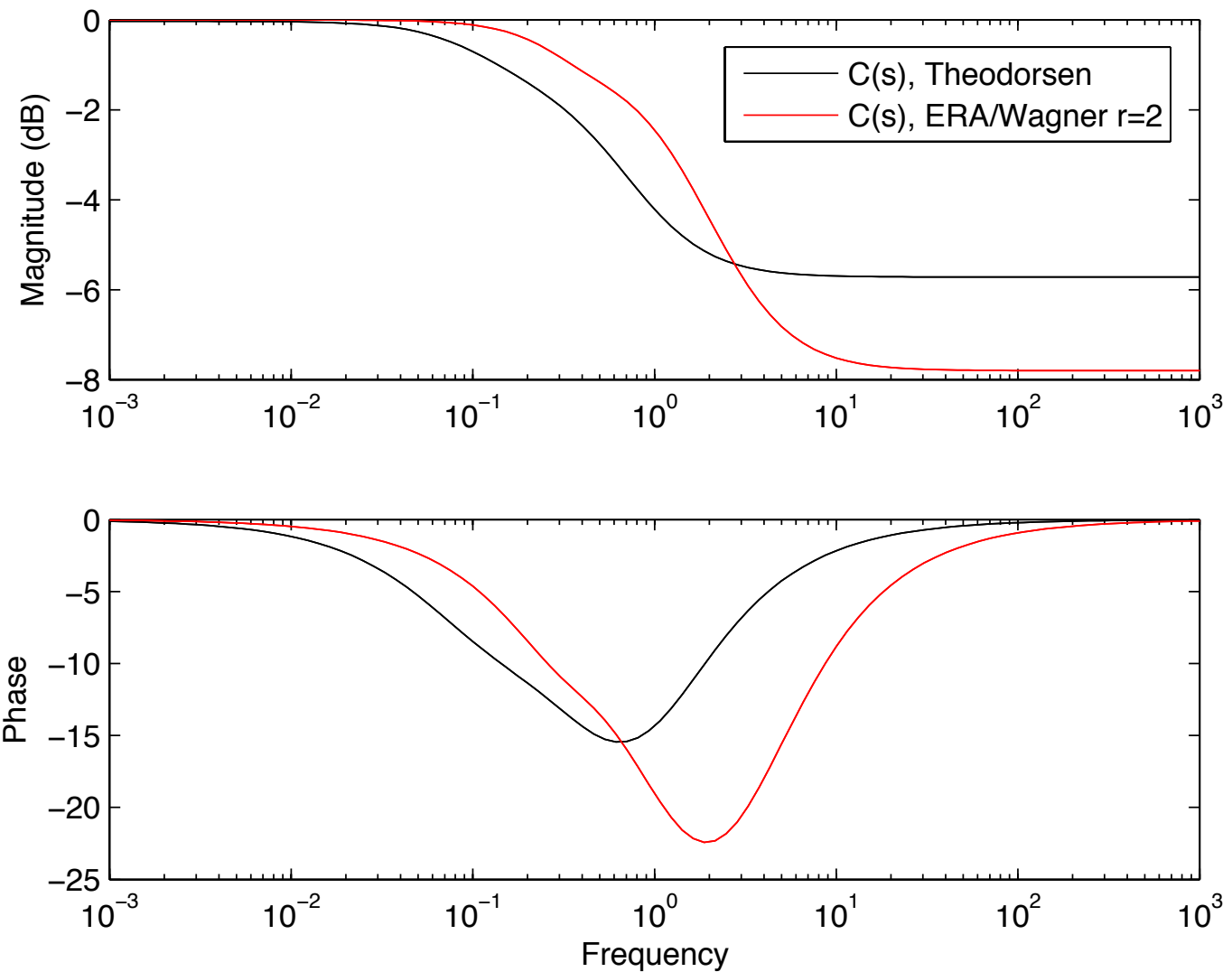


Isolating C(k)

Start with empirical ERA model

Subtract off quasi-steady and divide through by added-mass

Remainder is C(k)





Alternative Representation



Generalized Theodorsen

$$C_L = C_1 \left[\dot{\alpha} - \frac{a}{2} \ddot{\alpha} \right] + C_2 \left[\alpha + \frac{1}{2} \dot{\alpha} \left(\frac{1}{2} - a \right) \right] C(k)$$

$$C_L = \underbrace{-\frac{a}{2} C_1}_{C_{L\ddot{\alpha}}} \ddot{\alpha} + \underbrace{\left[C_1 + \frac{C_2}{2} \left(\frac{1}{2} - a \right) \right]}_{C_{L\dot{\alpha}}} \dot{\alpha} + \underbrace{C_2}_{C_{L\alpha}} \alpha - \underbrace{C_2 C'(k) \left[\alpha + \frac{1}{2} \dot{\alpha} \left(\frac{1}{2} - a \right) \right]}_{\text{fast dynamics}}$$

$$C_L(\alpha, \dot{\alpha}, \ddot{\alpha}, \mathbf{x}) = C_{L\alpha} \alpha + C_{L\dot{\alpha}} \dot{\alpha} + C_{L\ddot{\alpha}} \ddot{\alpha} + C \mathbf{x}$$

**Stability derivatives
plus fast dynamics**

State-Space Representation

$$\frac{d}{dt} \begin{bmatrix} x_1 \\ x_2 \\ \alpha \\ \dot{\alpha} \end{bmatrix} = \begin{bmatrix} -.6828 & -.0633 & C_2 & C_2(1-2a)/4 \\ 1 & 0 & 0 & 0 \\ 0 & 0 & 0 & 1 \\ 0 & 0 & 0 & 0 \end{bmatrix} \begin{bmatrix} x_1 \\ x_2 \\ \alpha \\ \dot{\alpha} \end{bmatrix} + \begin{bmatrix} 0 \\ 0 \\ 0 \\ 1 \end{bmatrix} \ddot{\alpha}$$

$$C_L = [.197 \quad .0303 \quad .5176C_2 \quad C_1 + .5176C_2(1-2a)/4] \begin{bmatrix} x_1 \\ x_2 \\ \alpha \\ \dot{\alpha} \end{bmatrix} - \frac{aC_1}{2} \ddot{\alpha}$$



Bode Plot of Theodorsen



$$C_L = \underbrace{\frac{\pi}{2} \left[\ddot{h} + \dot{\alpha} - \frac{a}{2} \ddot{\alpha} \right]}_{\text{Added-Mass}} + \underbrace{2\pi \left[\alpha + \dot{h} + \frac{1}{2} \dot{\alpha} \left(\frac{1}{2} - a \right) \right]}_{\text{Circulatory}} C(k)$$

$$k = \frac{\pi f c}{U_\infty}$$

Frequency response

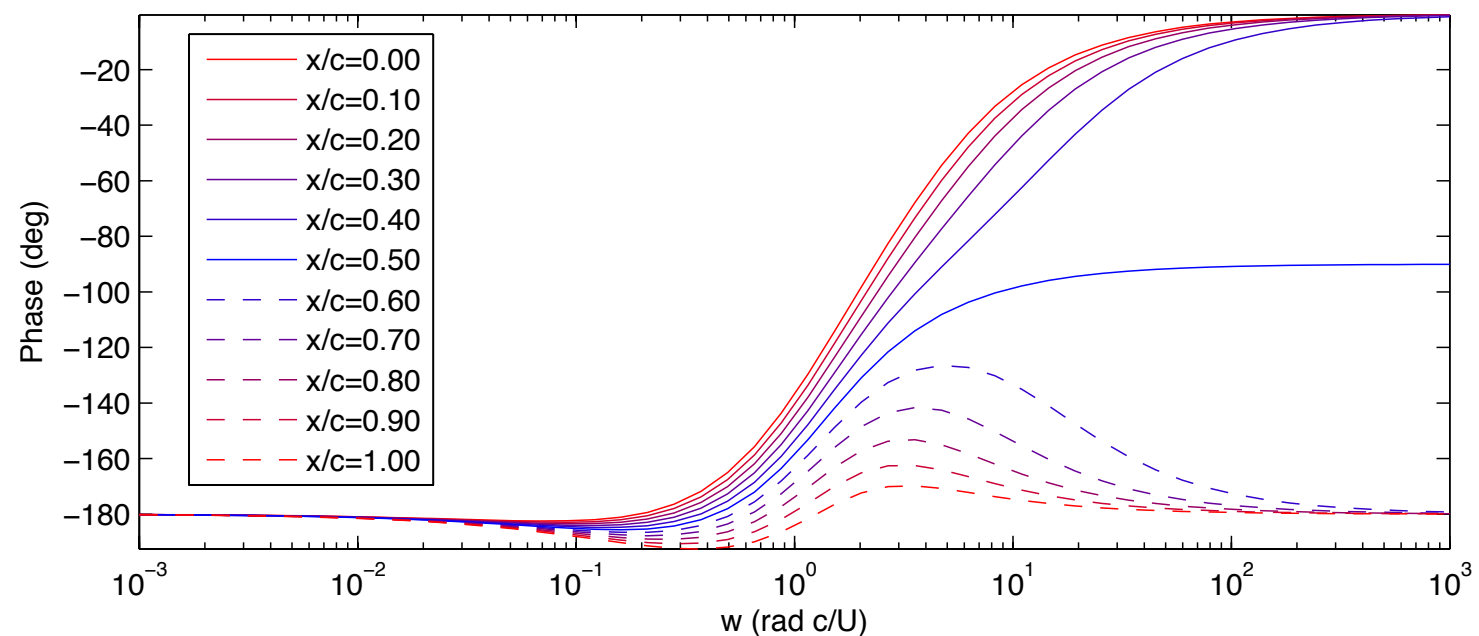
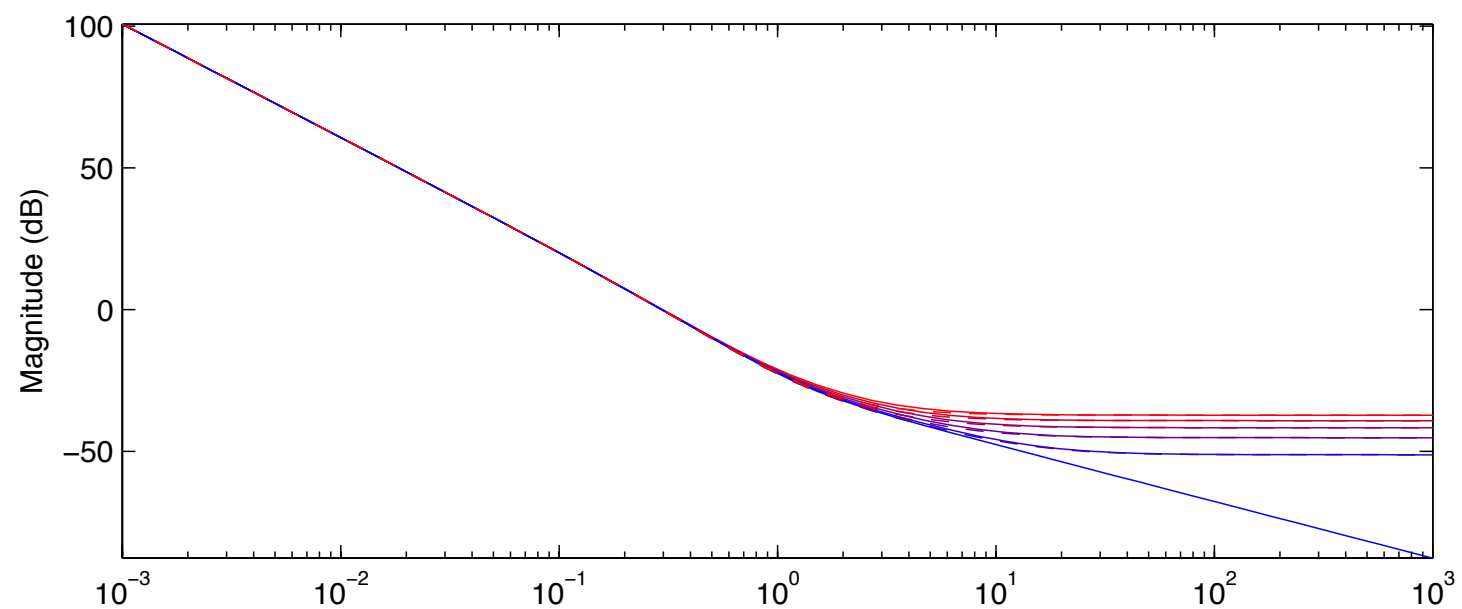
input is $\ddot{\alpha}$ (α is angle of attack)

output is lift coefficient C_L

Low frequencies dominated by quasi-steady forces

High frequencies dominated by added-mass forces

Crossover region determined by Theodorsen's function $C(k)$

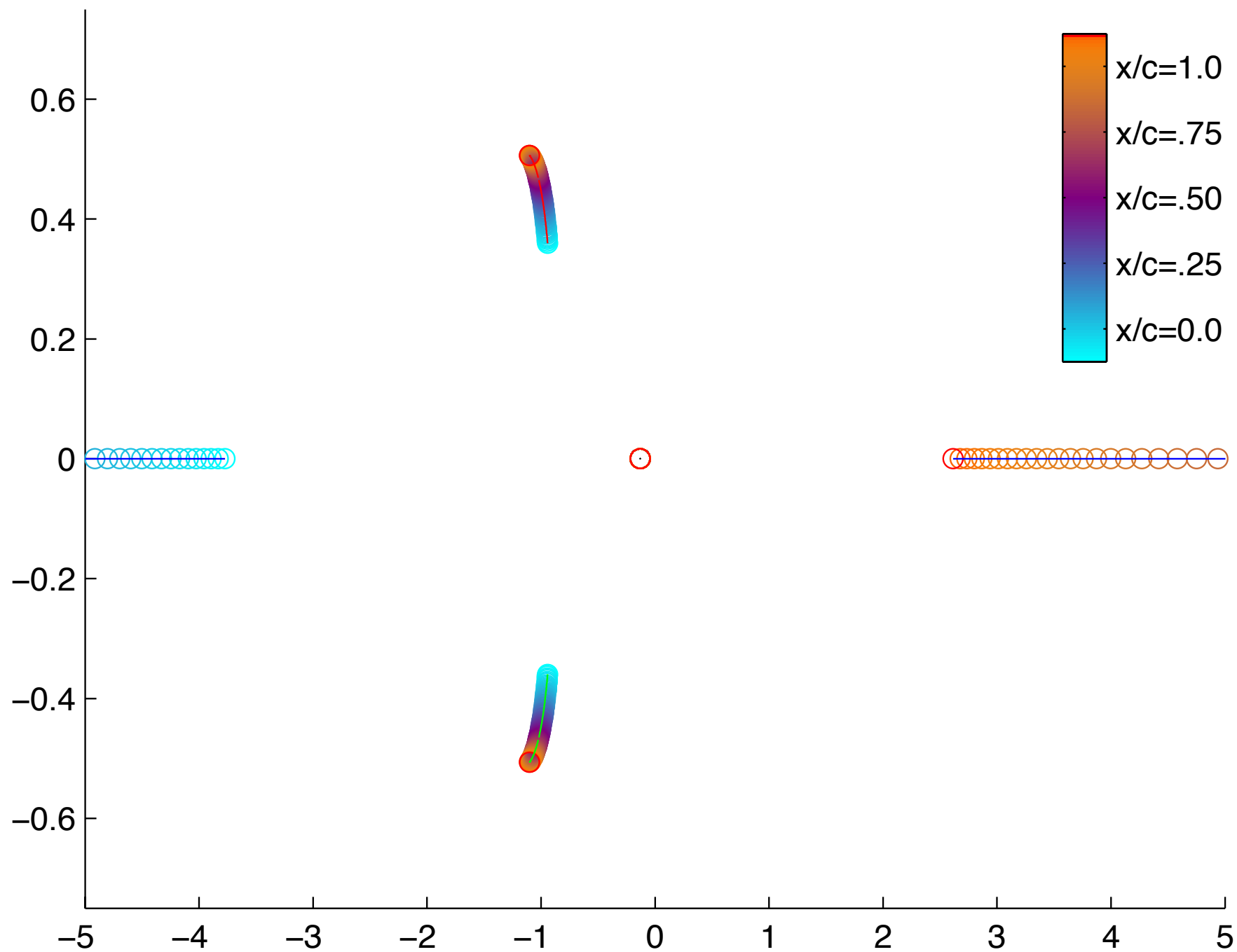




Zeros of Theodorsen's Model



Zeros of Theodorsen Model, Varying Pitch Point



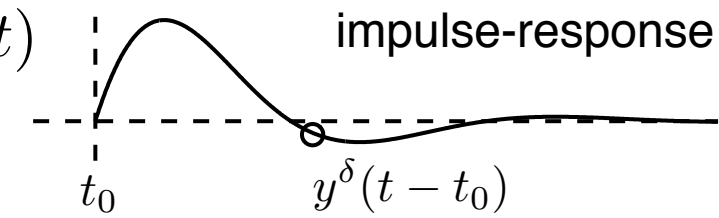
**As pitch point moves aft of center,
zero enters RHP at +infinity.**



Wagner's Indicial Response



Given an impulse in angle of attack, $\alpha = \delta(t)$, the time history of Lift is $C_L^\delta(t)$



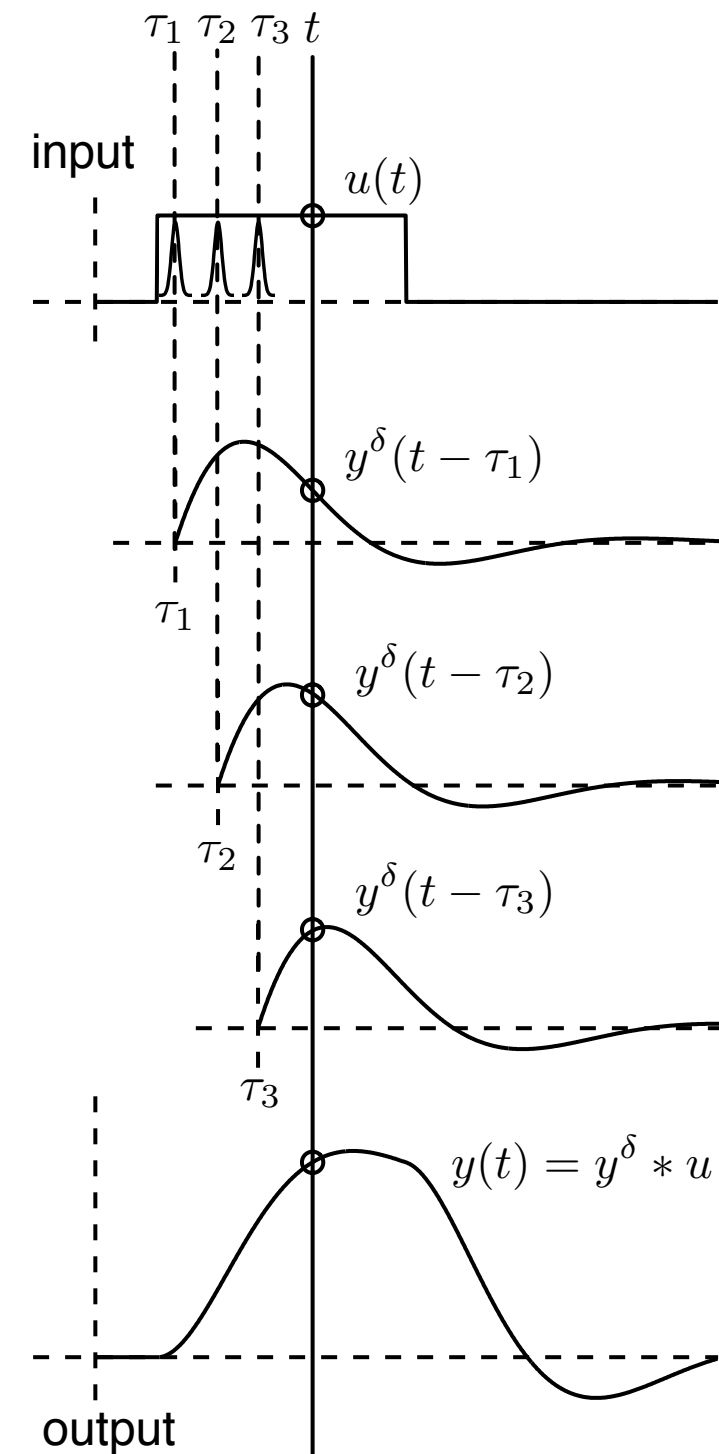
The response to an arbitrary input $\alpha(t)$ is given by linear superposition:

$$C_L(t) = \int_0^t C_L^\delta(t - \tau)\alpha(\tau)d\tau = (C_L^\delta * \alpha)(t)$$

Given a step in angle of attack, $\dot{\alpha} = \delta(t)$, the time history of Lift is $C_L^S(t)$

The response to an arbitrary input $\alpha(t)$ is given by:

$$C_L(t) = C_L^S(t)\alpha(0) + \int_0^t C_L^S(t - \tau)\dot{\alpha}(\tau)d\tau$$



Model Summary

Reconstructs Lift for arbitrary input

Linearized about $\alpha = 0$

Based on experiment, simulation or theory

convolution integral inconvenient for feedback control design

Wagner, 1925.

Leishman, 2006.



Reduced Order Wagner



**Stability derivatives
plus fast dynamics**

$$C_L(\alpha, \dot{\alpha}, \ddot{\alpha}, \mathbf{x}) = C_{L_\alpha} \alpha + C_{L_{\dot{\alpha}}} \dot{\alpha} + C_{L_{\ddot{\alpha}}} \ddot{\alpha} + C \mathbf{x}$$

Quasi-steady and added-mass

Fast
dynamics

Transfer Function

$$Y(s) = \left[\frac{C_{L_\alpha}}{s^2} + \frac{C_{L_{\dot{\alpha}}}}{s} + C_{L_{\ddot{\alpha}}} + G(s) \right] s^2 U(s)$$

State-Space Form

$$\frac{d}{dt} \begin{bmatrix} \mathbf{x} \\ \alpha \\ \dot{\alpha} \end{bmatrix} = \begin{bmatrix} A_r & 0 & 0 \\ 0 & 0 & 1 \\ 0 & 0 & 0 \end{bmatrix} \begin{bmatrix} \mathbf{x} \\ \alpha \\ \dot{\alpha} \end{bmatrix} + \begin{bmatrix} B_r \\ 0 \\ 1 \end{bmatrix} \ddot{\alpha}$$

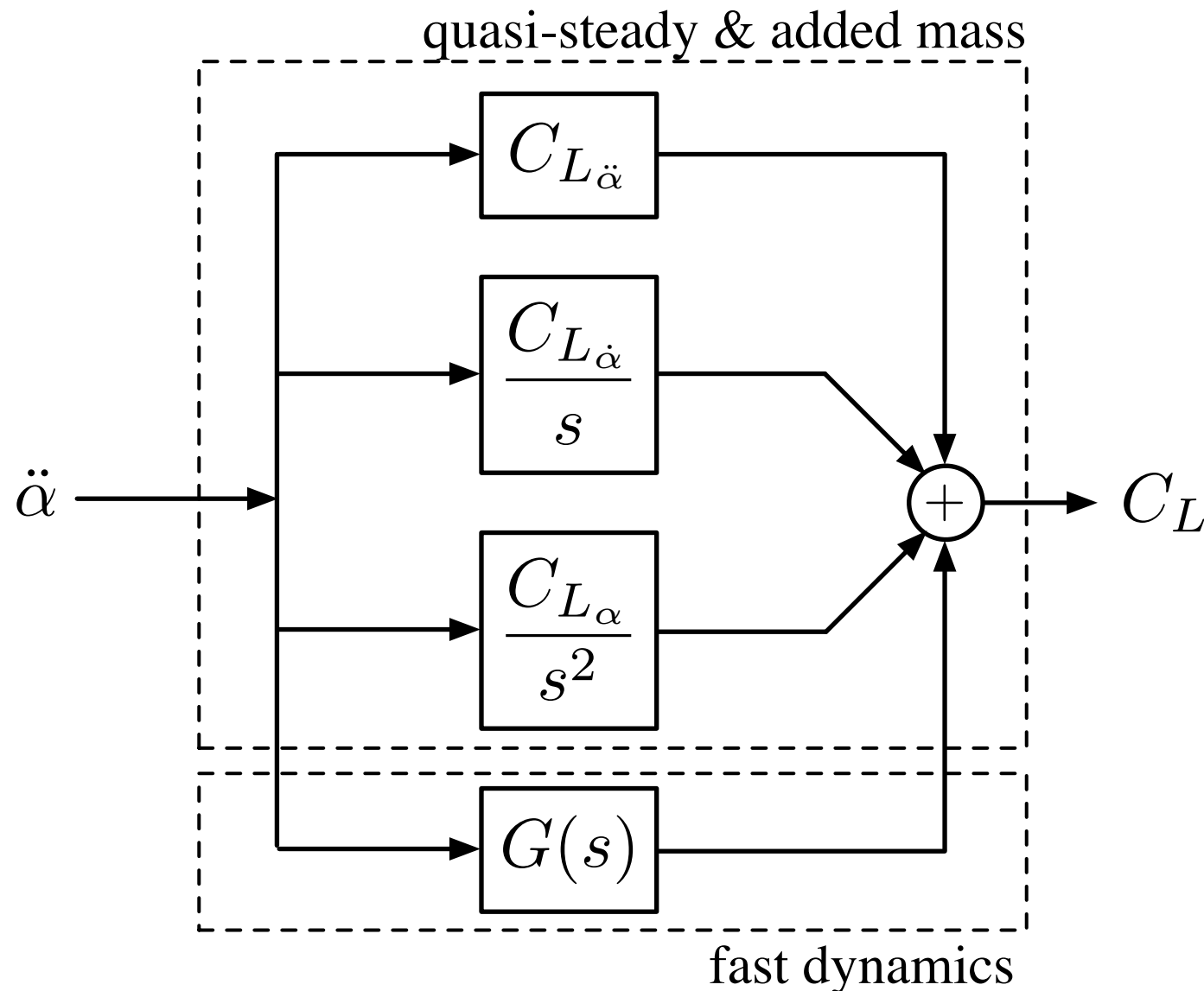
$$C_L = [C_r \quad C_{L_\alpha} \quad C_{L_{\dot{\alpha}}}] \begin{bmatrix} \mathbf{x} \\ \alpha \\ \dot{\alpha} \end{bmatrix} + C_{L_{\ddot{\alpha}}} \ddot{\alpha}$$



Reduced Order Wagner



$$C_L(t) = C_L^S(t)\alpha(0) + \int_0^t C_L^S(t - \tau)\dot{\alpha}(\tau)d\tau$$



fast dynamics

$$\frac{d}{dt} \begin{bmatrix} \mathbf{x} \\ \alpha \\ \dot{\alpha} \end{bmatrix} = \begin{bmatrix} A_r & 0 & 0 \\ 0 & 0 & 1 \\ 0 & 0 & 0 \end{bmatrix} \begin{bmatrix} \mathbf{x} \\ \alpha \\ \dot{\alpha} \end{bmatrix} + \begin{bmatrix} B_r \\ 0 \\ 1 \end{bmatrix} \ddot{\alpha}$$

input

$$C_L = [C_r \quad C_{L\alpha} \quad C_{L\dot{\alpha}}] \begin{bmatrix} \mathbf{x} \\ \alpha \\ \dot{\alpha} \end{bmatrix} + C_{L\ddot{\alpha}} \ddot{\alpha}$$

ERA Model

quasi-steady and added-mass

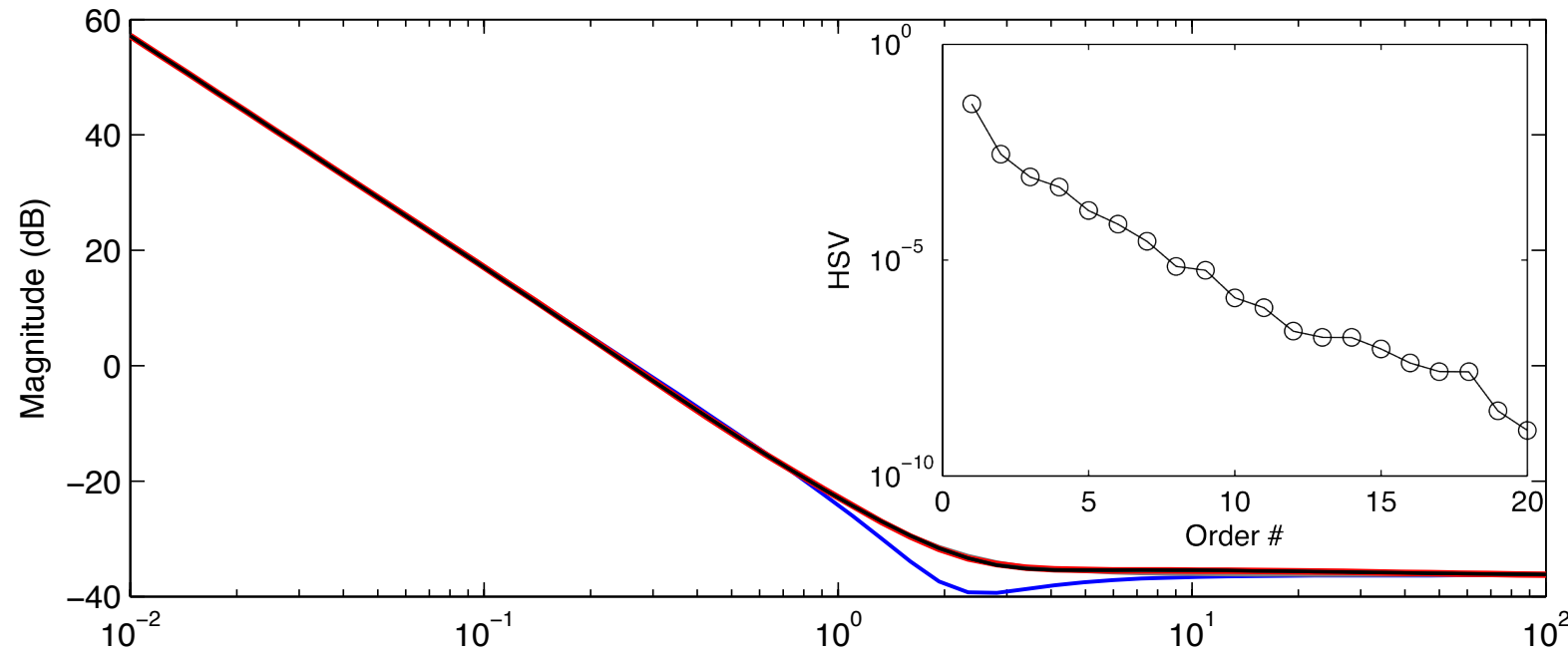
Model Summary

- Linearized about $\alpha = 0$
- Based on experiment, simulation or theory
- Recovers stability derivatives $C_{L\alpha}, C_{L\dot{\alpha}}, C_{L\ddot{\alpha}}$ associated with quasi-steady and added-mass

ODE model ideal for control design



Bode Plot - Pitch (LE)

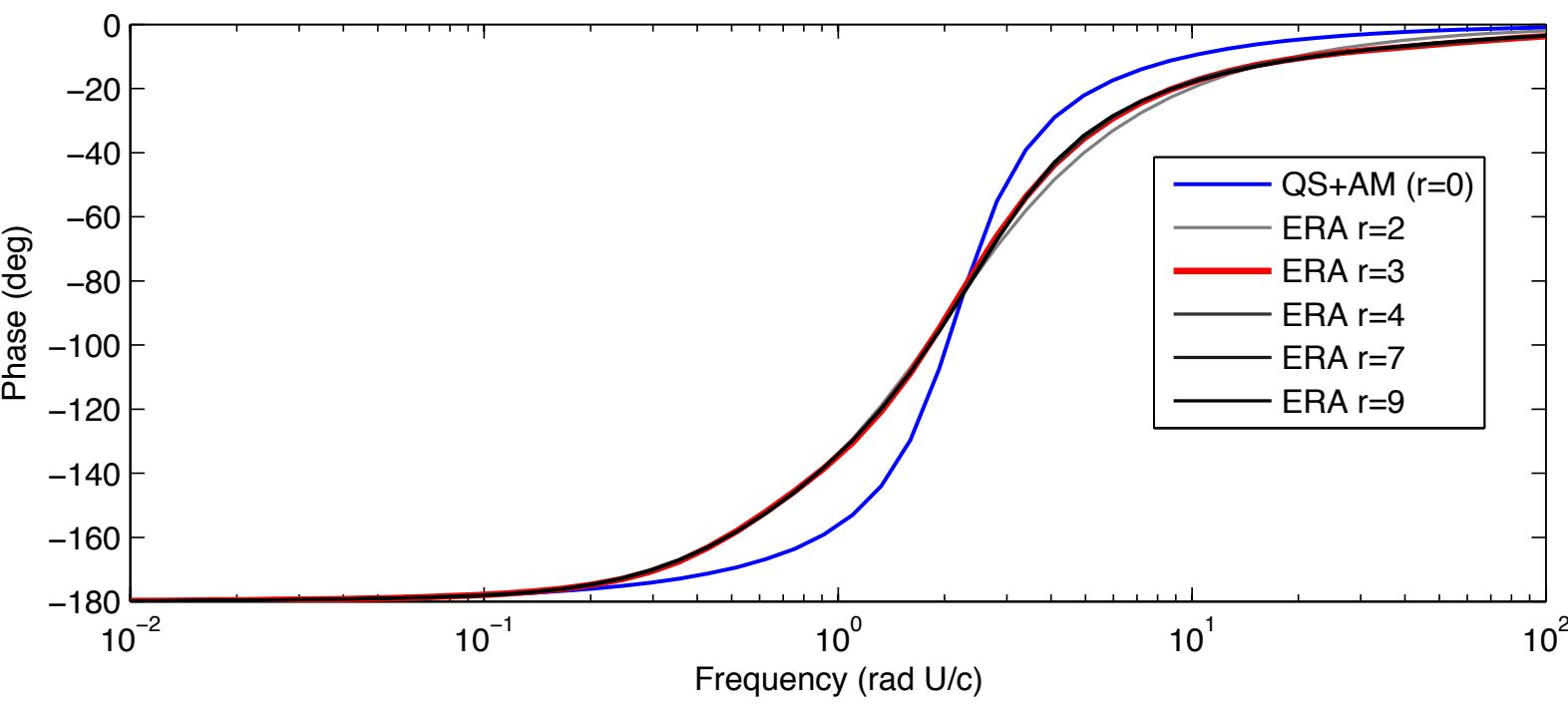


Frequency response

input is $\ddot{\alpha}$ (α is angle of attack)

output is lift coefficient C_L

Pitching at leading edge



Model without additional fast dynamics [QS+AM (r=0)] is inaccurate in crossover region

Models with fast dynamics of ERA model order >3 are converged

Punchline: additional fast dynamics (ERA model) are essential



Bode Plot - Pitch (QC)



Frequency response

input is $\ddot{\alpha}$ (α is angle of attack)

output is lift coefficient C_L

Pitching at quarter chord

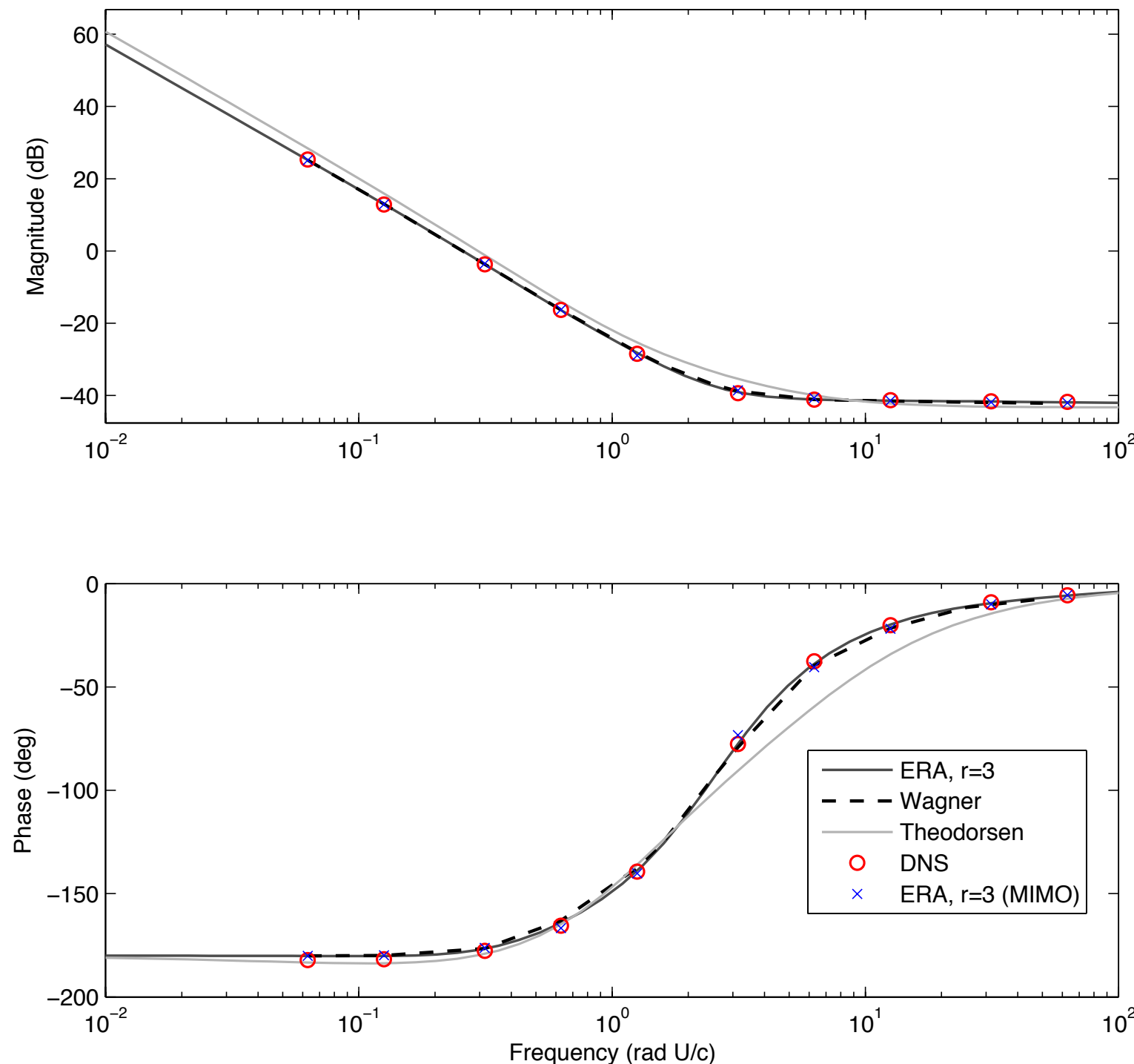
Reduced order model with ERA $r=3$
accurately reproduces Wagner

Wagner and ROM agree better with
DNS than Theodorsen's model.

Asymptotes are correct for Wagner
because it is based on experiment

Model for pitch/plunge dynamics
[ERA, $r=3$ (MIMO)] works as well,
for the same order model

Quarter-Chord Pitching

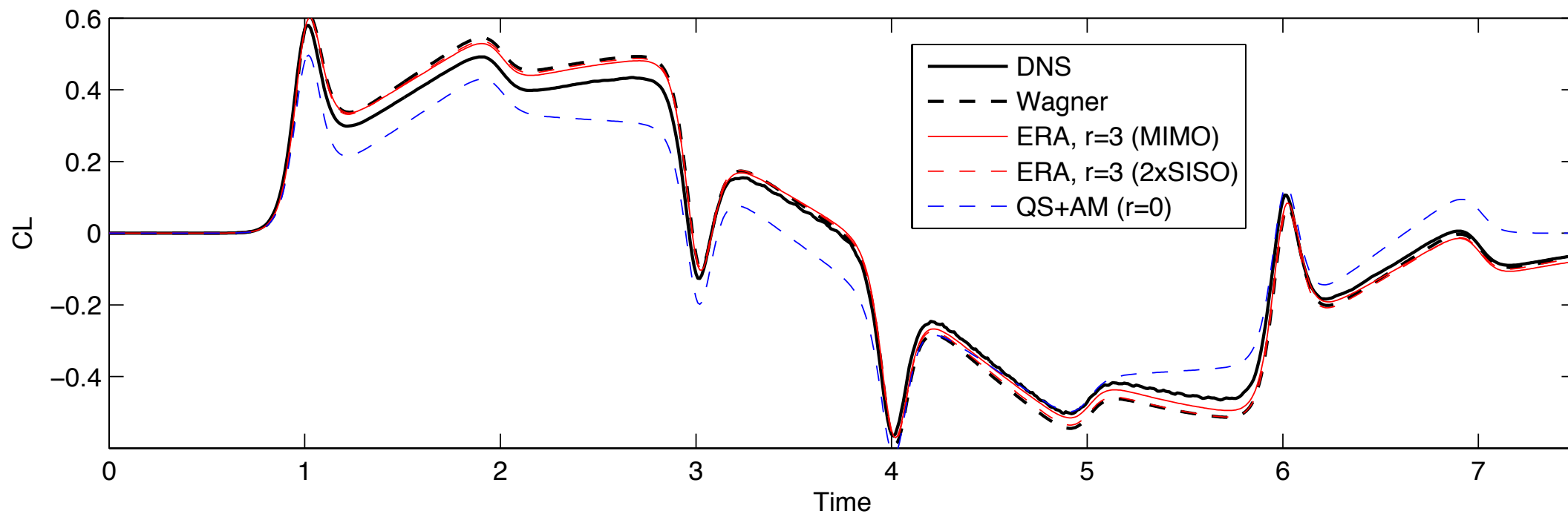
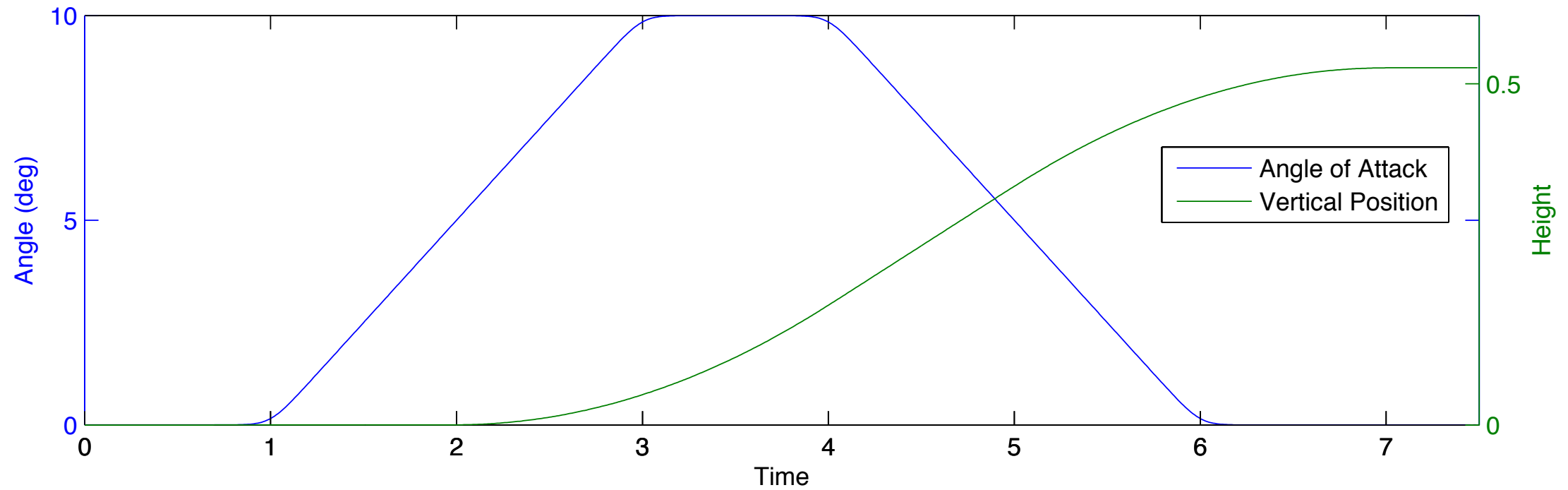




Pitch/Plunge Maneuver



Canonical pitch-up, hold, pitch-down maneuver, followed by step-up in vertical position

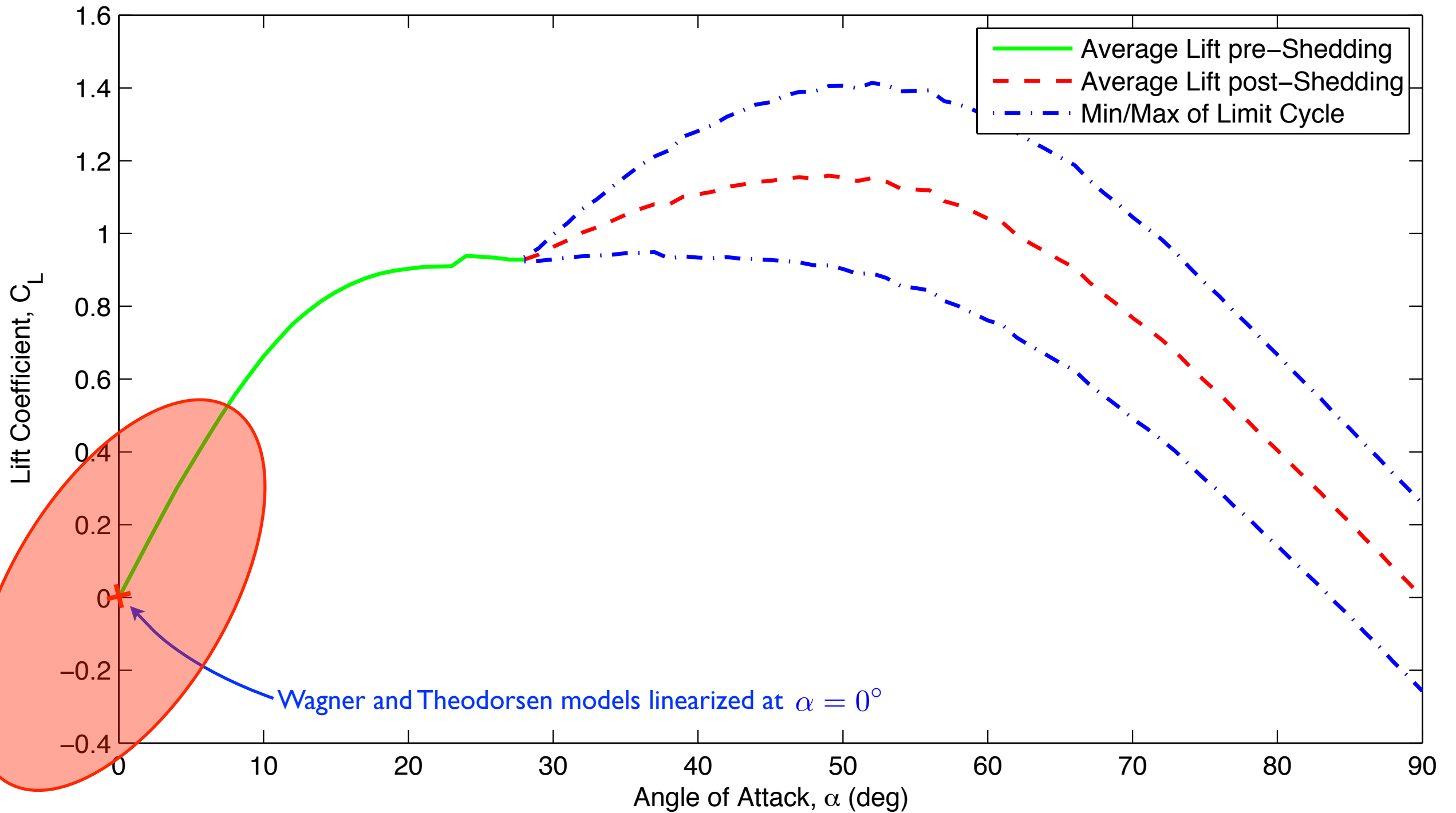


OL, Altman, Eldredge, Garman, and Lian, 2010
Brunton and Rowley, *in preparation*.

Reduced order model for Wagner's indicial response accurately captures lift coefficient history from DNS

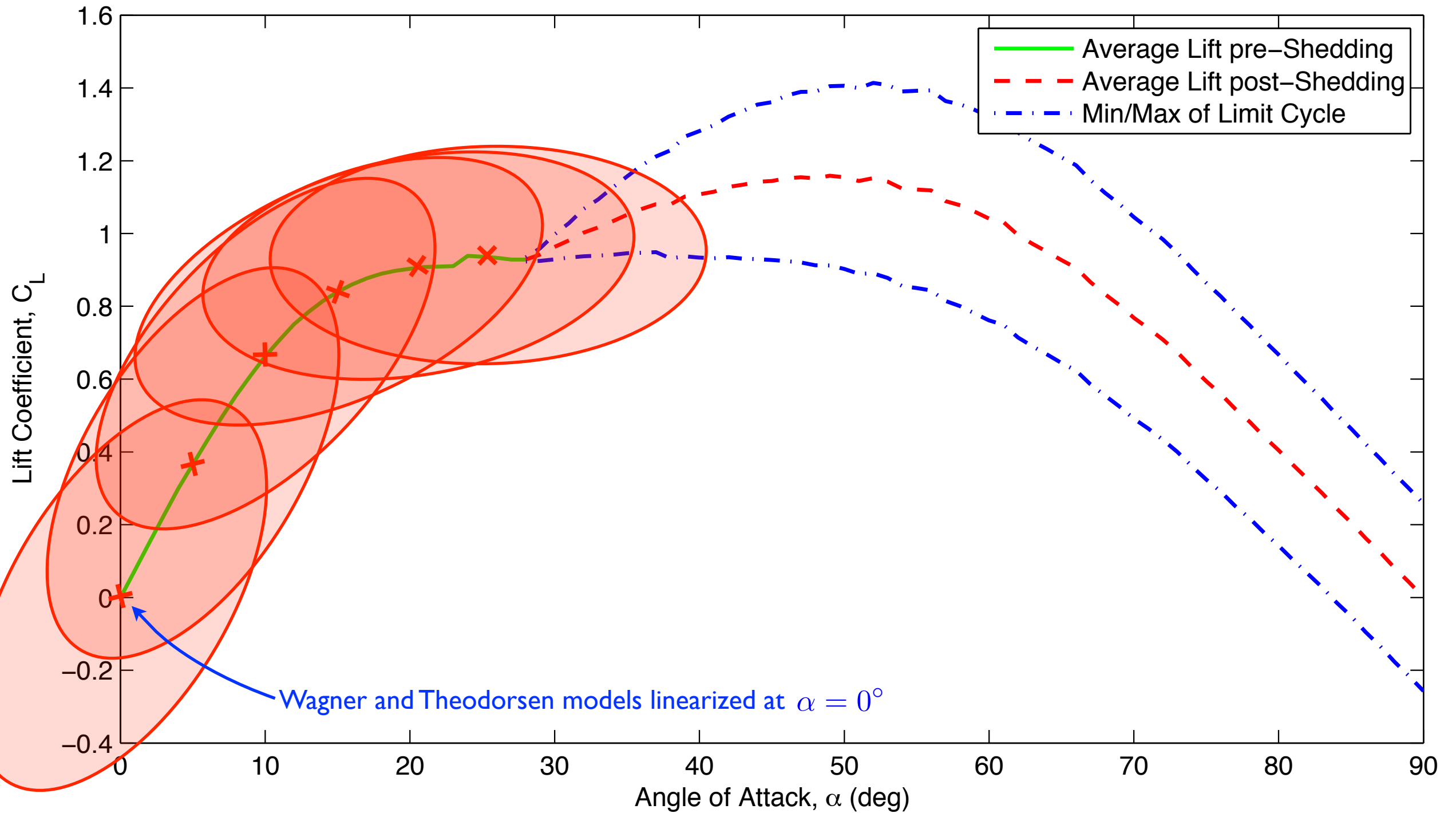


Lift vs. Angle of Attack





Lift vs. Angle of Attack





Bode Plot of ERA Models

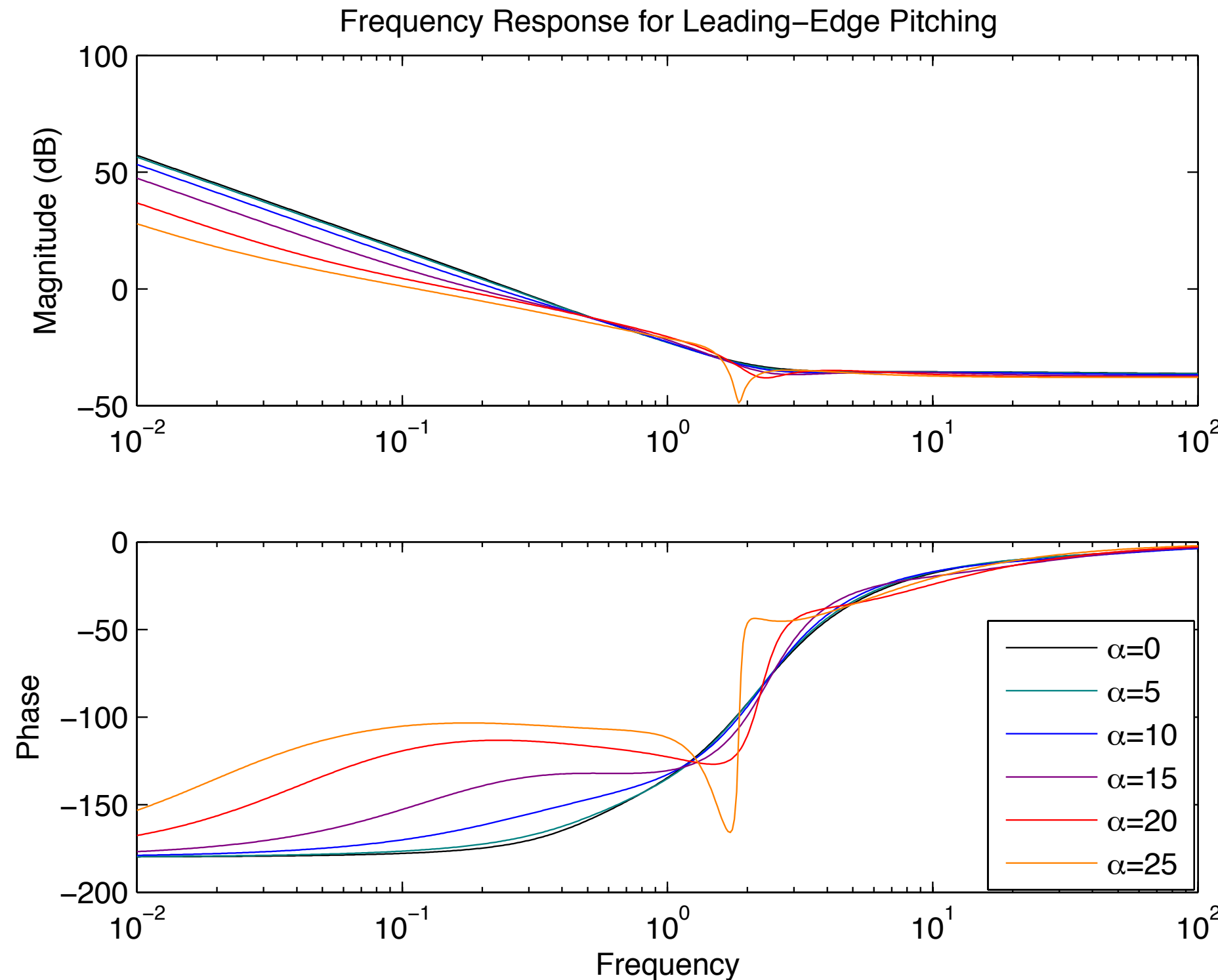


Results

Lift slope decreases for increasing angle of attack, so magnitude of low frequency motions decreases for increasing angle of attack.

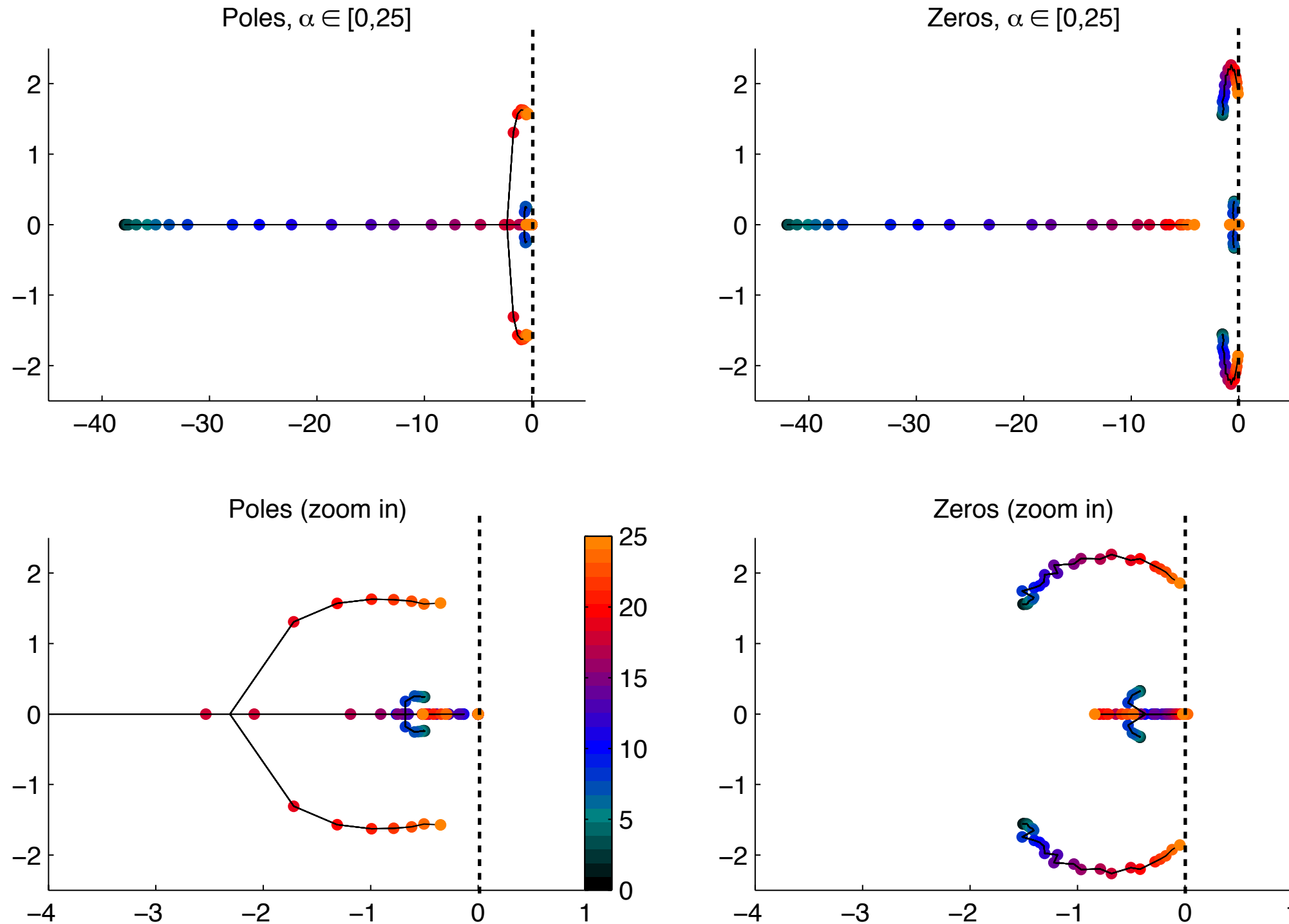
At larger angle of attack, phase converges to -180 at much lower frequencies. I.e., solutions take longer to reach equilibrium in time domain.

Consistent with fact that for large angle of attack, system is closer to Hopf instability, and a pair of eigenvalues are moving closer to imaginary axis.





Poles and Zeros of ERA Models

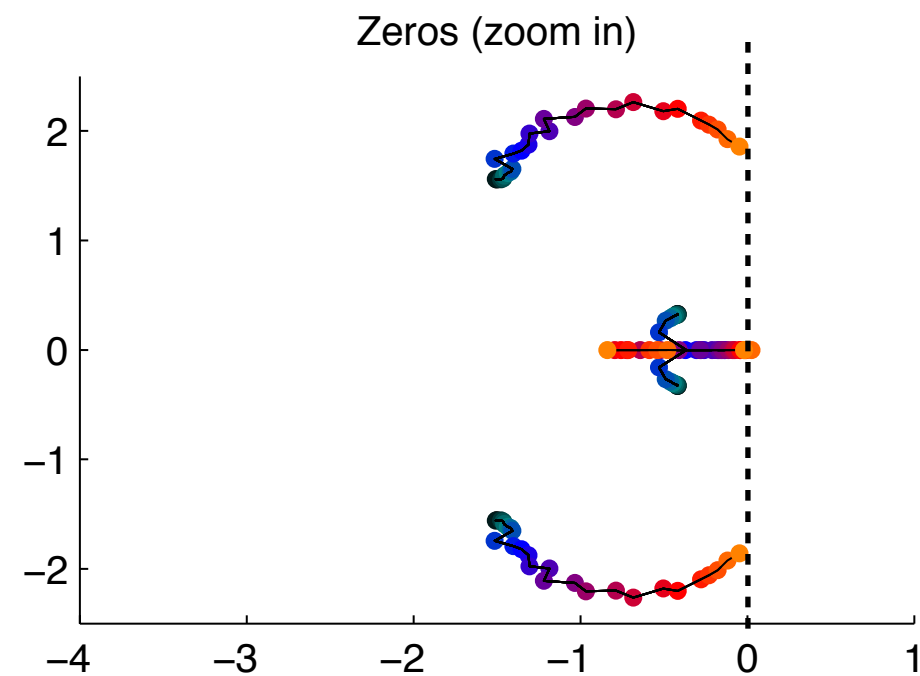
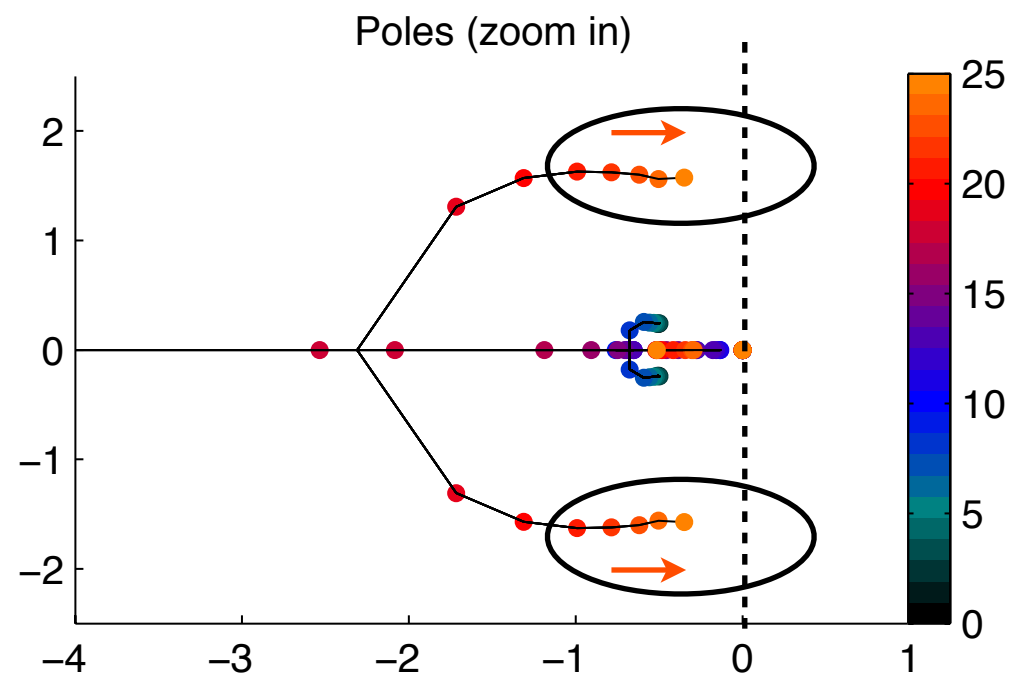
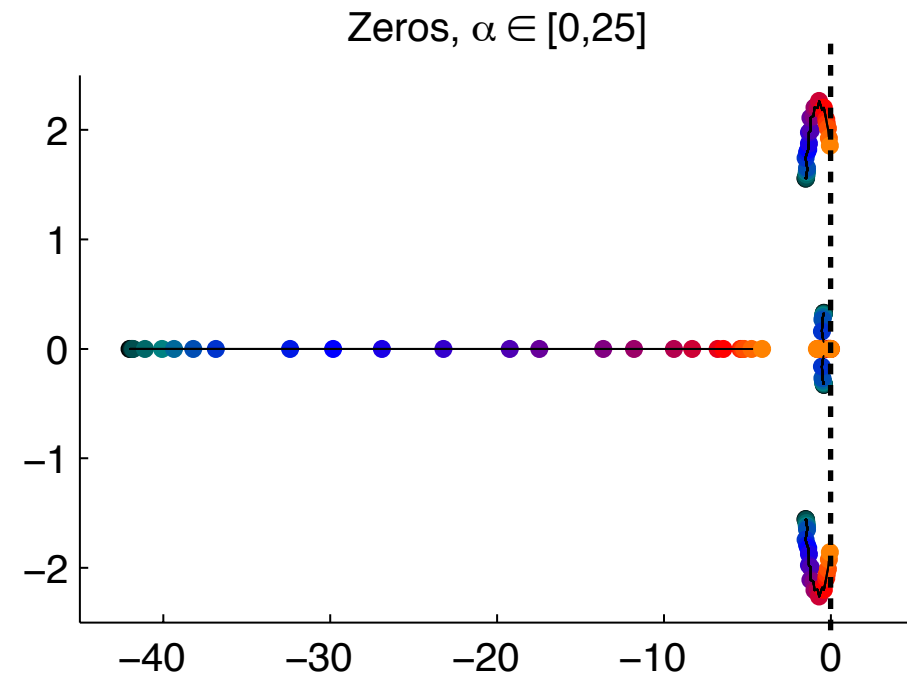
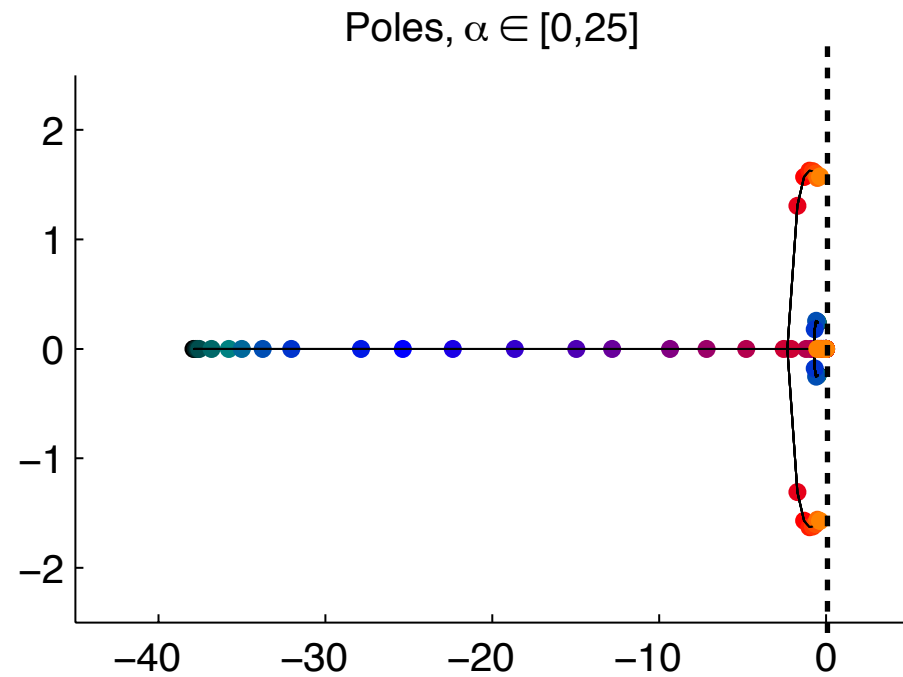


As angle of attack increases, pair of poles (and pair of zeros) march towards imaginary axis.

This is a good thing, because a Hopf bifurcation occurs at $\alpha_{\text{crit}} \approx 28^\circ$



Poles and Zeros of ERA Models

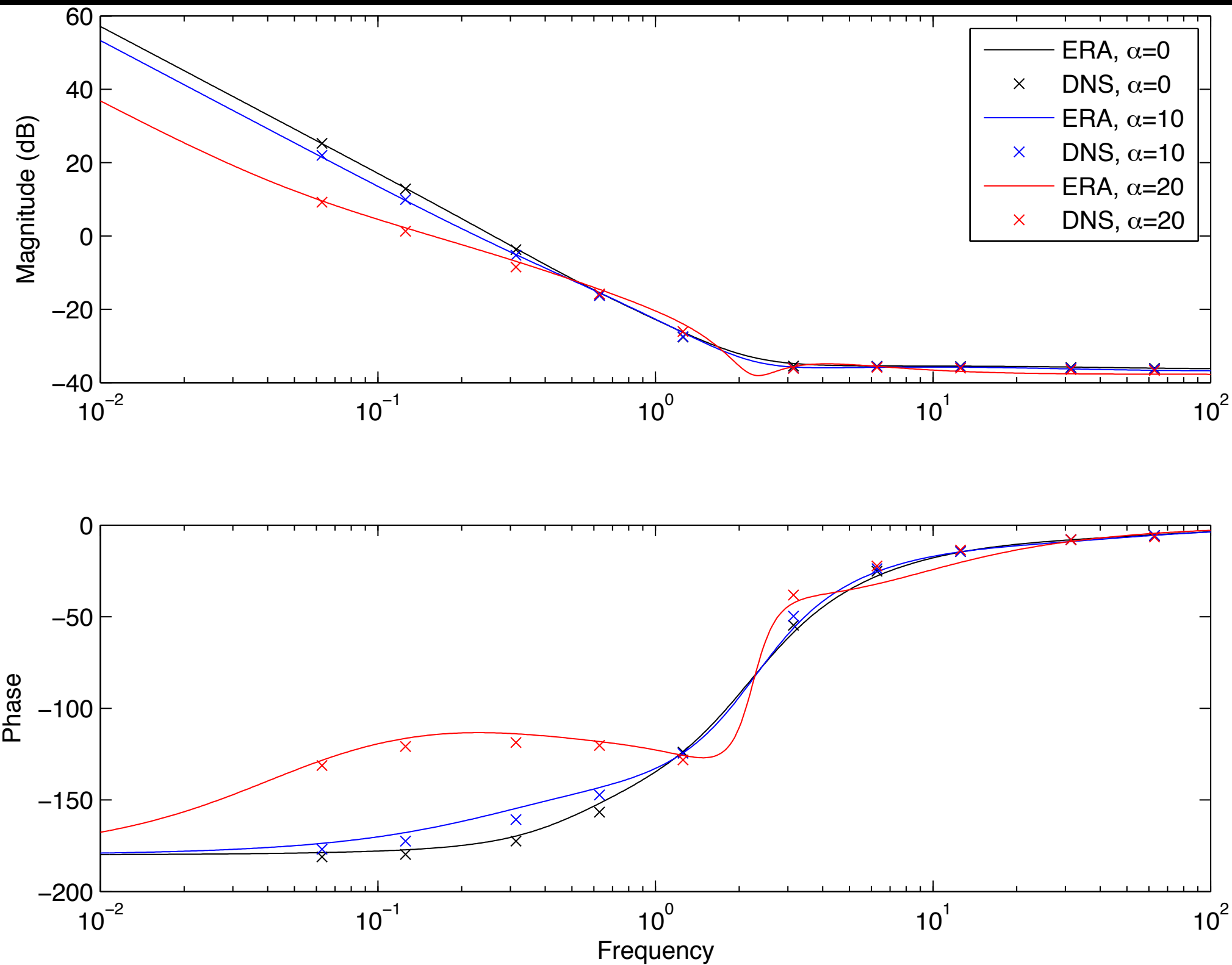


As angle of attack increases, pair of poles (and pair of zeros) march towards imaginary axis.

This is a good thing, because a Hopf bifurcation occurs at $\alpha_{\text{crit}} \approx 28^\circ$



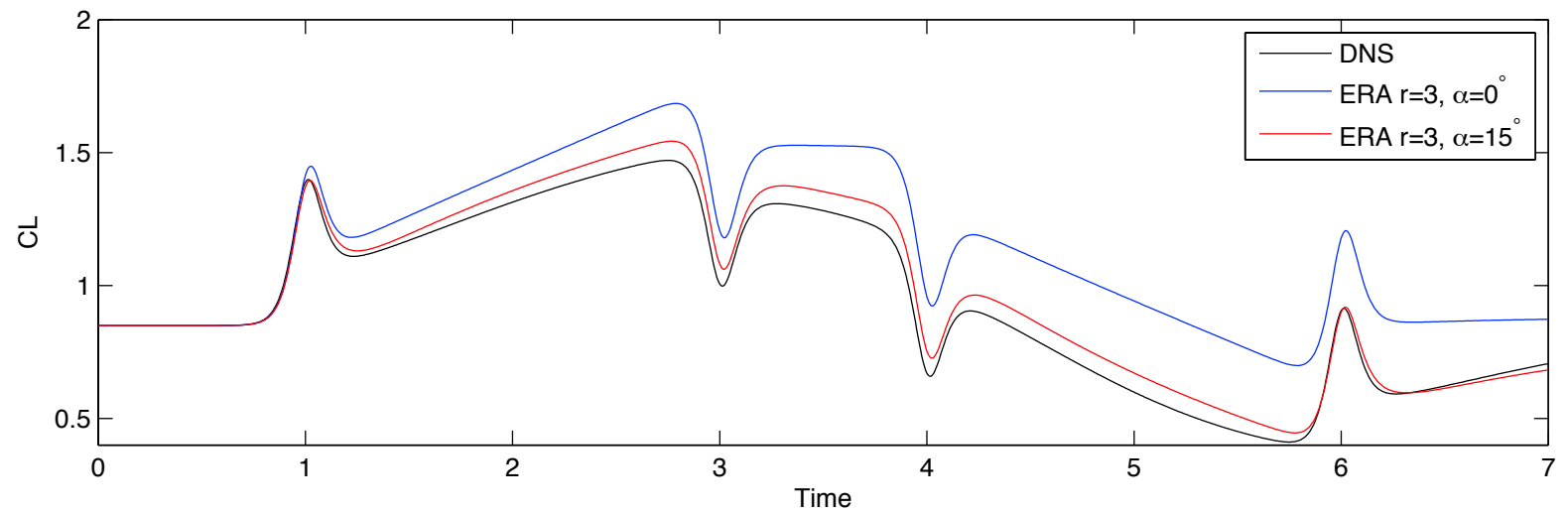
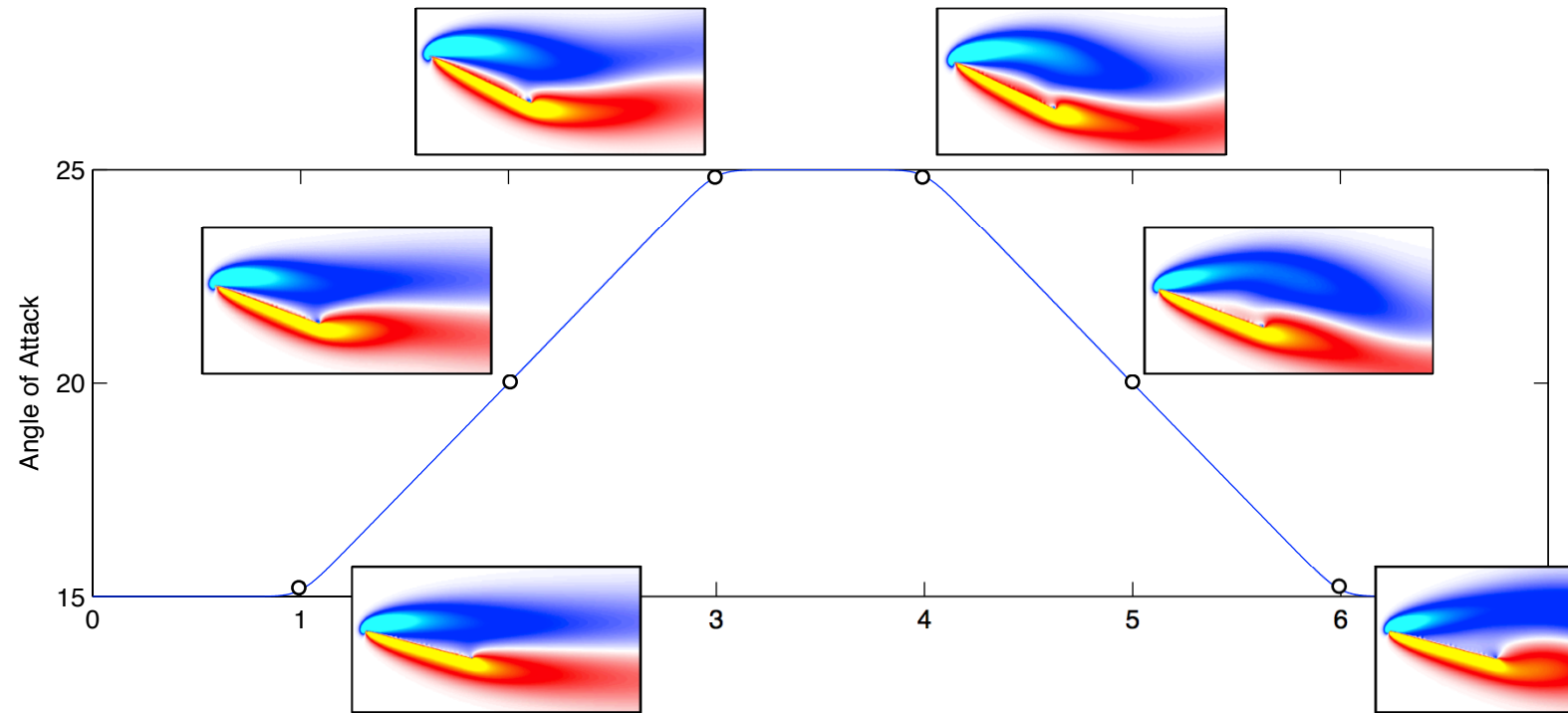
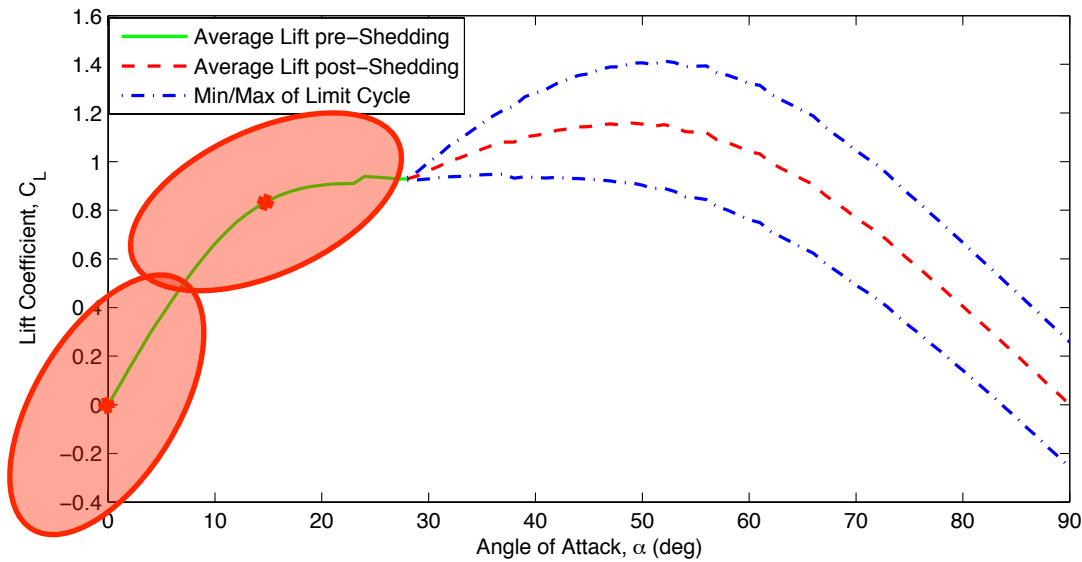
Bode Plot of Model (-) vs Data (x)



Direct numerical simulation confirms that local linearized models are accurate for small amplitude sinusoidal maneuvers



Large Amplitude Maneuver



Compare models linearized at

$$\alpha = 0^\circ \quad \text{and} \quad \alpha = 15^\circ$$

For pitching maneuver with

$$\alpha \in [15^\circ, 25^\circ]$$

Model linearized at $\alpha = 15^\circ$

captures lift response more accurately

$$G(t) = \log \left[\frac{\cosh(a(t - t_1)) \cosh(a(t - t_4))}{\cosh(a(t - t_2)) \cosh(a(t - t_3))} \right]$$

$$\alpha(t) = \alpha_0 + \alpha_{\max} \frac{G(t)}{\max(G(t))}$$



Conclusions



Reduced order model based on indicial response at non-zero angle of attack

- Based on eigensystem realization algorithm (ERA)
- Models appear to capture dynamics near Hopf bifurcation
- Locally linearized models outperform models linearized at $\alpha = 0^\circ$

Empirically determined Theodorsen model

- Theodorsen's $C(k)$ may be approximated, or determined via experiments
- Models are cast into state-space representation
- Pitching about various points along chord is analyzed

Future Work:

- Combine models linearized at different angles of attack
- Add large amplitude effects such as LEV and vortex shedding

Wagner, 1925.

Brunton and Rowley, AIAA ASM 2009-2011

Theodorsen, 1935.

OL, Altman, Eldredge, Garmann, and Lian, 2010

Leishman, 2006.

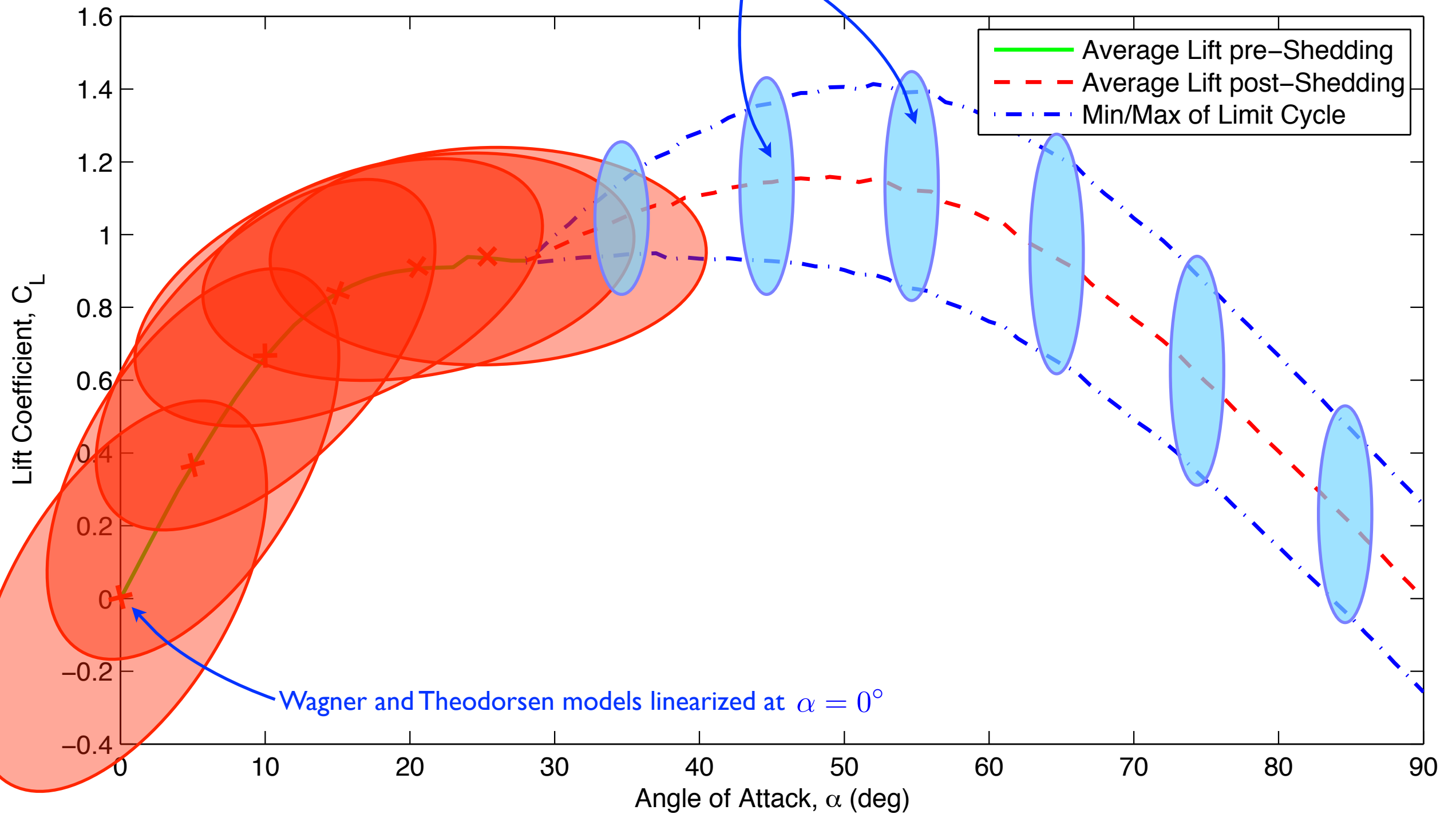
Breuker, Abdalla, Milanese, and Marzocca, AIAA 2008.



Lift vs. Angle of Attack



Models based on Hopf normal form capture vortex shedding





Bode Plot - Plunge



Frequency response

input is \ddot{y} (vertical acceleration)

output is lift coefficient C_L

Plunging changes flight path angle and free stream velocity

Reduced order model with ERA $r=3$ accurately reproduces Wagner

Wagner and ROM agree better with DNS than Theodorsen's model.

Asymptotes are correct for Wagner because it is based on experiment

Model for pitch/plunge dynamics [ERA, $r=3$ (MIMO)] works as well, for the same order model

Sinusoidal Plunging

